Universidad de Valladolid

CellMat Laboratory

FACULTY OF SCIENCE

CONDENSED MATTER PHYSICS DEPARTMENT

MASTER IN NANOSCIENCE AND MOLECULAR NANOTECHNOLOGY

ANALYSIS OF THE CROSS EFFECTS FOUND IN POLYMERIC CELLULAR MATERIALS FILLED WITH NANOADDITIVES. RELATIONSHIP BETWEEN DISPERSION AND FOAMABILITY.

Belén Notario Collado

Director:

Miguel Ángel Rodríguez Pérez

Analysis of the Cross Effects Found in Polymeric Cellular Materials Filled with Nanoadditives. Relationship between Dispersion and Foamability.

Acknowledgments **2**

1. Abstract **3**

2. Introduction **4**

2.1 Cellular Materials 4

2.2 Polymer Nanocomposites 7

2.3 Cellular Polymeric Nanocomposites 8

2.4 Processes for Producing Cellular Polymeric Materials 9

2.5 Nanofillers 11

2.6 Blowing Agents 14

2.7 Synchrotron Radiation for Energy Disperse X-Ray Diffraction (ED-XRD) 15

2.8 Bibliography 16

3. State of Art **19**

3.1 Dispersion/ Exfoliation of Nanoclays 19

3.2 Cellular Polyethylene/ Polystyrene Nanocomposites 20

3.3 Bibliography 22

4. Objectives **24**

5. Experimental **25**

5.1 Materials and Sample Preparation 25

5.2 Characterization of Solid Nanocomposites 29

5.3 Characterization of Cellular Nanocomposites 30

5.4 Bibliography 33

6. Results and Discussions **34**

6.1 In-Situ Characterization of the Foaming Process in PE/ MMT System 34

6.2 Characterization of Dispersion in the PS/ Sepiolite System 41

7. Conclusions **49**

8. Future Work **52**

ACKNOWLEDGMENTS

I would like to thank Prof. Dr. Miguel Ángel Rodríguez Pérez his daily support, his trust and advice. Without him, this Master Thesis would have not been possible.

Financial support from the University of Valladolid and Banco Santander with an FPI grant is gratefully acknowledged.

1. ABSTRACT

Today´s society demands lightweight materials with tailor-made properties for each application. Cellular materials, due to the weight, cost and raw material reduction and the excellent properties that can be achieved with their use, have a great present and a promising future in important technological sectors such as automotive, aeronautics, rail, renewable energies, the marine industry, etc. However, nowadays there is a lack of knowledge in various aspects of the science and technology of these materials that is limiting the production and development of new and better products. A new step, in this sense, is the development of cellular materials in which the polymer matrix incorporates nanoparticles. In the last years, efforts have been focused on this topic.

This Master Thesis is focused on two specific research topics related to the use of nanoparticles in cellular polymers:

1. The first one is connected to the in-situ monitoring of the exfoliation process of one kind of nanoclays (montmorillonite) in a polyethylene matrix during foaming with chemical blowing agents.

2. The second line aims at studying the dispersion of another kind of nanoclays (sepiolites) in a polystyrene matrix and its effectiveness as nucleating agent. These results will be compared with the ones obtained from talc, the typical particle used as nucleating agent in the production of low density polystyrene foams.

Cellular materials have been produced using two different techniques: free foaming (where azodicarbonamide, hydrocerol and expancel will be used as chemical foaming agents) and the batch gas dissolution foaming process with CO_2 as physical blowing agent.

2. INTRODUCTION

2.1 CELLULAR MATERIALS

A polymeric cellular material consists of two phases: one continuous macromolecular solid phase and other either continuous or discontinuous gaseous phase [1].

Within cellular materials are found materials with a regular structure and materials with a stochastic structure (see Figure 1).

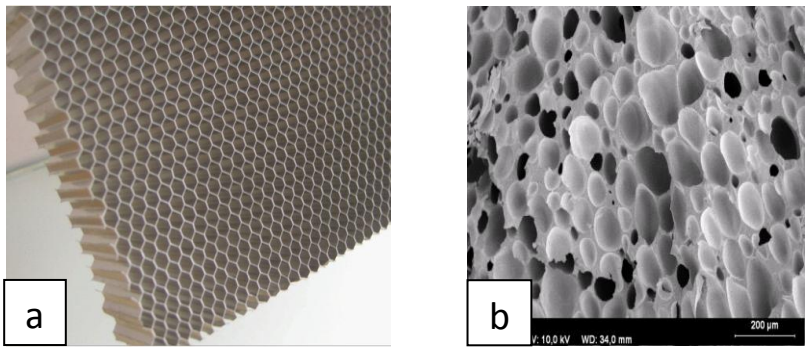

Figure 1: a) Material with a regular structure (honeycomb). b) Material with a stochastic structure (polymer foam).

Secondly, another classification of cellular materials is connected with their structure. One can distinguish between open cell cellular materials and closed cell cellular materials (see Figure 2). In the case of open cell (Figure 2a), cells are interconnected, being the gas phase continuous. However, in closed cell (Figure 2b), the gas is confined within the cells without any continuity, only the solid phase is continuous [1, 2]. Intermediate situations can also occur where both types of cells coexist (Figure 2c), generally due to fractures of the cells walls in closed cell cellular materials, acquiring, therefore, a certain degree of open cell fraction.

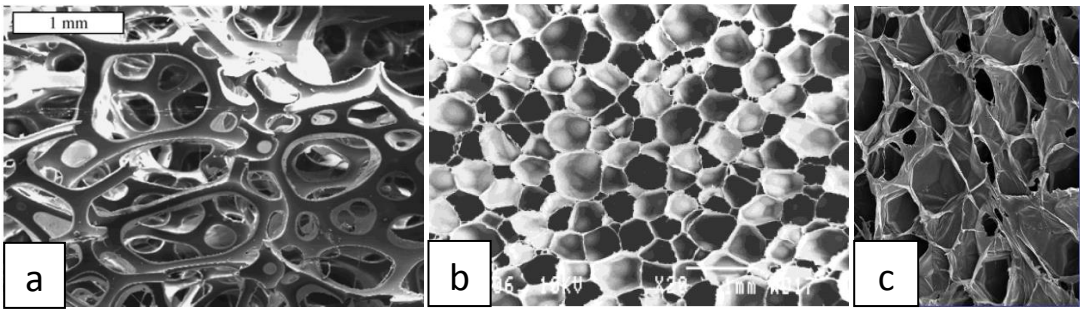

Figure 2: a) Open cell cellular structure. b) Closed cell cellular structure. c) Partially open cell cellular structure.

A third classification of cellular materials can be performed taking into account their density [1, 3]. Density is a fundamental parameter because it determines both the properties as the field of application of these materials.

The concept of relative density is often used [1, 3]. It expresses the ratio between the cellular material density and the former solid precursor (Eq. 1). Besides, another quite useful

quantitative relation can be established defining the expansion grade (EG) [1, 3] as the inverse value of the relative density. This parameter expresses the volume ratio of the cellular material in comparison with the one of the initial precursor (Eq. 2).

$$\rho_{relative} = \frac{\rho_{cellular\ material}}{\rho_{solid}} \qquad \text{Eq. 1}$$

$$EG = \frac{1}{\rho_{relative}} = \frac{\rho_{solid}}{\rho_{cellular\ material}} \qquad \text{Eq. 2}$$

It can be distinguished between high density cellular materials ($\rho_{relative} > 0.6$), medium density cellular materials ($0.3 < \rho_{relative} < 0.6$) and low density cellular materials ($\rho_{relative} < 0.3$) [3].

There is a strong dependence of the properties of cellular materials with its density. Any property can be estimated taking into account the scale relations [1, 4, 5]. These are a set of empirical equations that relate a certain property of the cellular material with the property that the solid material would have, taking into account both the solid density (ρ_{solid}) and the density of the cellular product ($\rho_{cellular\ material}$):

$$P_{cellular\ material} = C \cdot P_{solid} \left(\frac{\rho_{cellular\ material}}{\rho_{solid}}\right)^n \qquad \text{Eq. 3}$$

Where *C* usually takes values close to 1 and *n* varies in between n = 1 and n = 2 depending on the cellular structure and the property under study. Both are determined experimentally. If a reduction of properties as small as possible is required, it is necessary to generate cellular structures giving values of *n* close to 1 [1, 5, 6].

Finally, in the case of polymeric cellular materials, a new classification of the cellular materials can be done considering the polymer matrix or based polymer used [7, 8]. There are three types of polymeric matrices:

- Elastomers: These materials may be subjected to large deformations without causing its rupture and also have the ability to spontaneously recover the original shape when the force origin of the deformation ceases. Examples of these materials include polybutadiene, natural rubber, EPDM, etc.
- Thermoset: These materials are subjected to a curing process which produces the crosslinking of the polymer chains that cannot be melted. Examples of thermosetting materials are polyurethane and epoxy resins.
- Thermoplastic: They are linear or branched polymers that can be softened by applying heat. They are characterized by a not fully crystallized structure when they are cooled from its molten state. Many of these materials are semi-crystalline, i.e. consist of two phases: an amorphous one, characterized by presenting no long range atomic order,

and a crystal one having such arrangement. Examples of thermoplastics are polyethylene, polypropylene, polystyrene, PVC, etc.

From the technical point of view, cellular materials spread the range of properties of their respective dense solids (Figure 3). For instance, mechanical properties can be improved at equivalent weight (better specific stiffness) in bending tests. Concerning thermal properties, it can be remarked that they also present better insulating capabilities providing lower thermal conductivities.

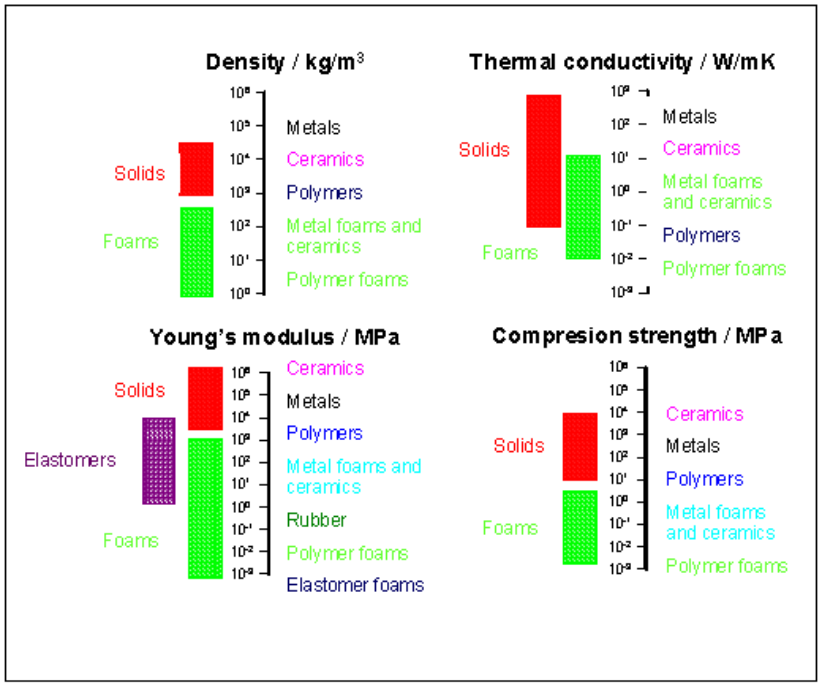

Figure 3: Comparison of typical values of density, modulus of elasticity, thermal conductivity, and compressive strength corresponding to metals, polymers, ceramics and cellular solids with different matrices, polymer, metal and ceramic.

Cellular structure and properties are intimately related in a polymeric cellular material and, thus it is important to control processing parameters aiming to control the cellular structure with the objective of achieving a final specific compliance.

The properties of a cellular material depend on its density, but also on its cellular structure and on the properties of the polymer matrix comprising cell walls [1, 3, 6, 9, 10]. Hence, the design of cellular materials implies the optimization of materials at all these levels.

2.2 POLYMER NANOCOMPOSITES

Polymer nanocomposites are relatively a new generation of materials formed by a polymer matrix to which nanoparticles have been added. Nanoparticles are characterized by having, at least, one dimension in the nanometer range and can be of three types: laminar (nanoclays and graphenes), tubular (nanofibers and carbon nanotubes) or spherical (particles of silica or titanium oxide, among others).

The inclusion of nanofillers as reinforcement in conventional systems is nowadays a "hot topic" aiming at the developing new advanced and tailored materials with improved mechanical, thermal or even electrical properties [11, 12, 13]. The introduction of small amounts of well-dispersed nanoadditives to traditional materials gives as a result nanocomposites, which may present synergistic effects, not only summing the advantages of the conventional material and nanoadditives, but also yielding to new and/ or superior final properties [14].

Some of the most significant effects that can be achieved by introducing nanoparticles in the polymer matrix are among others the modification of the morphology and the rheological behavior of the polymer, improvements in thermal, mechanical, barrier or flame resistant properties (Figure 4).

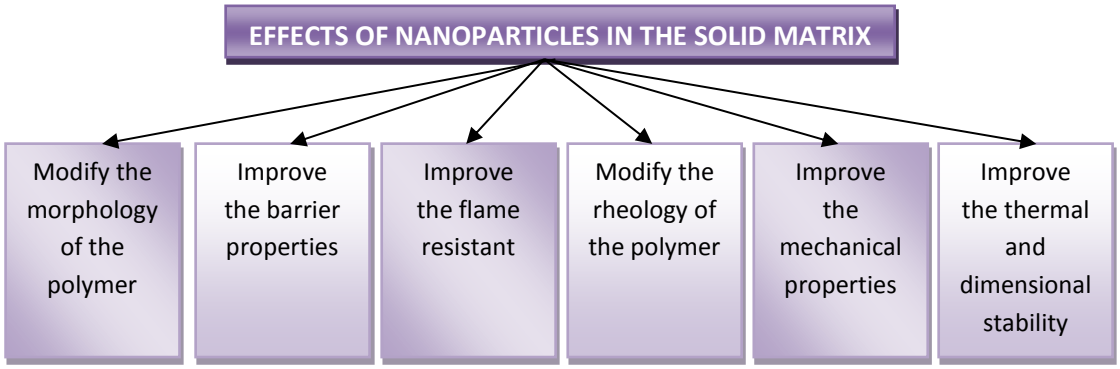

Figure 4: Effects of nanoparticles in the solid matrix.

The key aspect of nanoparticles is their high specific surface, so when they are adequately dispersed in the polymer matrix can lead to higher levels of improvements than when conventional micro sized fillers are used.

However, to get all the aforementioned properties a high degree of dispersion of the nanoparticles in the polymer matrix is needed, besides a good degree of compatibility between the nanoparticle and the polymer. A high agglomeration ratio or a poor compatibility may cause the obtaining of worst properties in the nanocomposites than in the neat polymer [15].

Carbon nanotubes, graphene layers, glass and carbon fibers, fullerenes, metal oxides or nanoclays are potential fillers recently developed, and are being used to produce these new nanocomposites not only in polymeric matrices, but also in metals, semiconductors or ceramic [16, 17, 18].

2.3 CELLULAR POLYMERIC NANOCOMPOSITES

In the last years the emergence of nanocomposites has resulted in the development of a new group of materials known as cellular polymeric nanocomposites. Foamed polymeric nanocomposites are currently subject of attention in both the scientific and industrial communities. The combination of functional nanoparticles and foaming technologies has a high potential to generate a new class of materials that are light weight, high strength and multifunctional [19].

To obtain an optimized cellular material the particles should act at two levels: on the one hand, improving the cellular structure and on the other hand optimizing the base polymer properties. Nanoparticles are capable of acting at these two levels, on the one hand increasing the properties of the polymer that form the cell walls in the way mentioned in the previous section (Figure 3), and on the other hand helping to generate improved cellular structures. The effects that nanoparticles have in the production process of a cellular material are summarized in Figure 5.

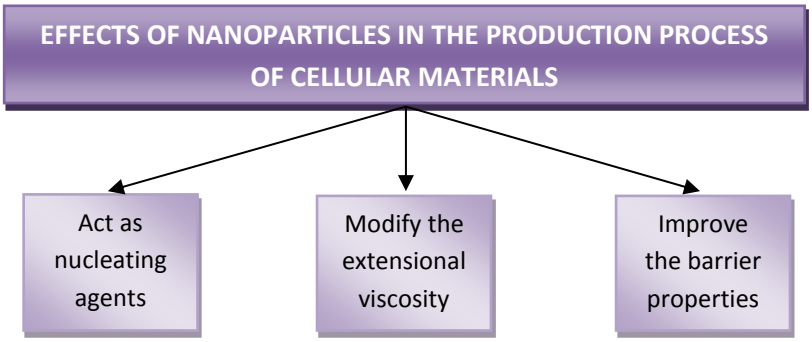

Figure 5: Effects of nanoparticles in the production process of a cellular material.

Firstly, nanoparticles could act as nucleating agents decreasing the energy needed by a cell to nucleate and be formed during the foaming process [20]. In the last years, as with the polymer composites, the size of the fillers used in polymer foams has been reduced from the micrometer to the nanometer range. The reason is simple, using the same nominal percentage of nanoparticles and considering that are well distributed, the number of potential nucleation sites per unit volume available is higher than when bigger particles are used [14]. In addition, nanoparticles produce an increase in the nucleation rate. The elevated superficial area of the nanoparticles favors the generation of a large interphase polymer-particle. The presence of such interphase could reduce the activation energy needed in the nucleation process of a cell producing an increase in the nucleation rate [14].

Secondly, it is considered that nanoparticles can contribute to reduce both the coalescence and the percentage of open cells in the material [14, 19]. The addition of nanoparticles to a polymer is also sometimes associated with a change in extensional viscosity. In some cases, if the particles are oriented in the stretching direction, it can be observed Strain Hardening in the polymer. The presence of the Strain Hardening phenomenon in the polymer matrix favors the stabilization of the cellular structure reducing phenomena such as coalescence or coarsening,

as it improves the ability of the polymer to retain gas during the expansion process of the material.

Finally, nanoparticles increase barrier properties of the polymer causing a higher difficulty for the gas phase to escape during foaming. When the polymer is foamed this can be translate into a higher capacity of the polymer to retain the gas.

Nevertheless, obtaining of all these effects depends on multiple factors such as the shape of the nanoparticle (laminar, tubular or spherical), the percentage of the nanoparticles added to the polymer, the kind of superficial treatment of the fillers, the degree of dispersion of the particles along the polymer matrix and the compatibility polymer-matrix [21-22].

The reasons exposed in the previous paragraphs justify that the combination of both types of materials, polymer nanocomposites and cellular materials, could present synergetic effects which are important to achieve excellent physical properties and significant weight reductions.

2.4 PROCESSES FOR PRODUCING CELLULAR POLYMERIC MATERIALS

The choice of one process or another is mainly determined by the type of polymer, by the final density of the foamed material, by the shape of the part to be manufactured and by the kind of cellular structure that it should present [3,6].

In general, most foaming processes are focused on the generation of a polymer/gas dissolution as homogeneous as possible. The control of parameters such as pressure, time or temperature is fundamental in most of the foaming processes.

Some of the most common processes for producing cellular polymeric materials are free foaming, extrusion, compression molding, improved compression molding, injection molding and batch gas dissolution foaming process.

In this work cellular materials are manufactured using two different techniques: free foaming (using different chemical blowing agents) and batch gas dissolution foaming process (using CO_2 as a physical blowing agent). These two techniques are briefly described as follows:

- Free foaming

  Prior to the foaming, the polymer is melt blended with a chemical blowing agent whose decomposition temperature is higher than the melting temperature of the polymer, forming a solid precursor.

  The foaming process itself consists of one stage. The solid precursor is foamed by heating the material in a furnace up to a temperature above the decomposition temperature of the blowing agent. In this process, firstly the polymer begins to melt and secondly, when the temperature of decomposition of the chemical blowing agent is reached, the gas is released allowing the nucleation and growth of the cells and

leading to the final foam. Normally, the foam reaches a maximum expansion and later collapses [3, 6]. Foaming temperature and foaming time are the key parameters to control the cellular structure of the final product.

- Batch gas dissolution foaming process.

  It is a two-steps process; first of all the polymer is saturated with supercritical CO_2 at high pressure and low temperature, in a glassy state. Next, the polymer/gas mixture is quenched into a supersaturated state by reducing drastically the pressure. Finally, after removing rapidly the sample from a CO_2 vessel, polymer is foamed by heating to a temperature above the glass transition temperature (e.g. in a hot bath or in a furnace as in our case), leading to nucleation and cell growth. Foaming temperature and foaming time are the key parameters to adjust the cellular structure of the final product [23, 24]. Using this process, microcellular foams using polymeric matrices such as polystyrene [25], polypropylene [26, 27], polyethersulfone and polyphenylsulfone [28, 29], polycarbonate [30], poly (methyl methacrylate) [31] and biodegradable poly (lactic acid) have been prepared. The use of CO_2 is due to its chemical, environmental, and economical advantages with respect to other gases and the high solubility of this gas in polymers.
  Foaming of polymers with gases or supercritical fluids allows the successful production of microcellular polymers. Such structures consist of pores with diameter smaller than 10 µm and cell densities larger than 10^9 cells per cm^3 [32]. Compared to solid materials, these foams exhibit significant advantages. They offer reduced bulk density that induces materials' saving and decreases transportation cost. On the other hand, they often exhibit high impact strength, high toughness, high stiffness-to-weight ratio, high fatigue life as well as low dielectric constant and low thermal conductivity [32]. These unique properties indicate microcellular polymers as candidate materials for many industrial applications, which include aircraft and automotive parts, sporting equipment, acoustic dampening, thermal insulation, microelectronic applications and optical devices [33]. Furthermore, foaming of polymers with gases or supercritical fluids exhibits a strong advantage especially in the processing of polymers for various biomedical applications. There is no need for use of harmful organic solvents that in most cases are not easily removed from the final product material.

2.5 NANOFILLERS

According to their shape, there are three major types of nanofillers: round, elongated and platelet-like nanofillers [14, 34]. This classification is established on the basis of how many dimensions at nanoscale they present. Nanoparticles such as spherical silica have all three dimensions at the nanometer scale, fibers belong to the elongated type nanofillers that show two dimensions at nanoscale and clays are representative of platelet-like nanofillers where only the thickness is in the range of few nanometers.

Among all the mentioned types, the main nanofillers used today are natural nanoclays, which are relatively inexpensive, commercial available, exhibiting layered morphology with high aspect ratio, large specific surface areas and that can cause an improvement in the mechanical properties of polymers, assuring a correct polymer-filler interaction [35, 36].

Two different nanofillers, in particular, two different types of nanoclays, are used in this work: montmorillonite and sepiolite.

Montmorillonite is a 2:1 clay, meaning that it has 2 tetrahedral sheets sandwiching a central octahedral sheet (Figure 6).

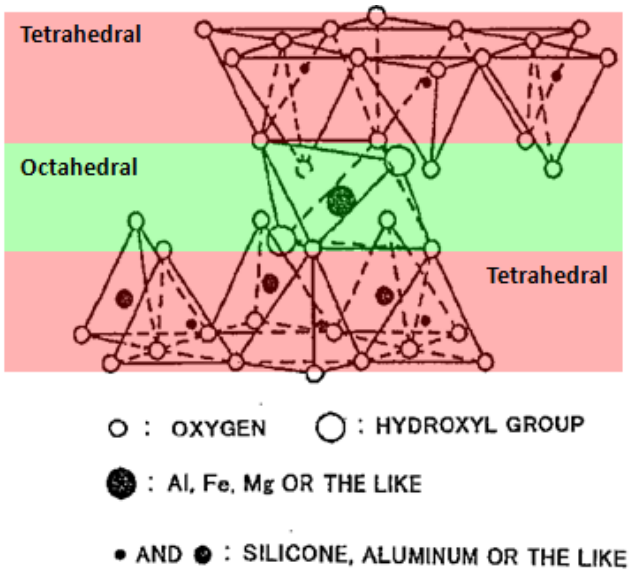

Figure 6: Montmorillonite structure

Chemically it is hydrated sodium calcium aluminium magnesium silicate hydroxide $(Na,Ca)_{0.33}(Al,Mg)_2(Si_4O_{10})(OH)_2{\cdot}nH_2O$.

Montmorillonite is used in the oil drilling industry as a component of drilling mud, as a soil additive to hold soil water in drought prone soils, to the construction of earthen dams and levees and to prevent the leakage of fluids. It is also used as a component of foundry sand and as a desiccant to remove moisture from air and gases.

The tetrahedral + octahedral + tetrahedral assembly is commonly called platelet. These platelets are agglomerated together by hydrogen bonding forces forming micron sized structures. Some commercially nanoclays are typically treated with quaternary ammonium

salts, a process called "organofilización" (Figure 7). These quaternary ammonium salts are introduced between platelets separating them slightly and decreasing hydrogen bonding attractions. At this time we would say that nanoclay is slightly intercalated.

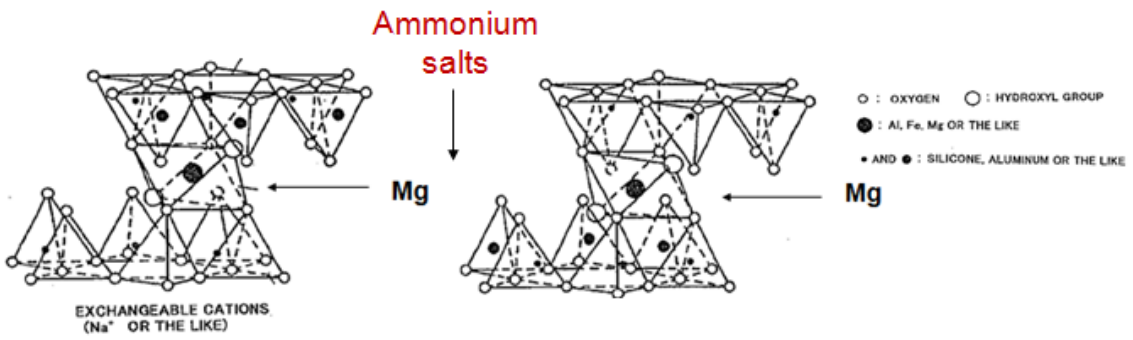

Figure 7: Organofilización process

The final goal is to exfoliate this nanoclay because of the reasons exposed above (see section “Polymer Nanocomposites”). Exfoliation process would consist in the separation of all these platelets. These individual platelets would have nanometric dimensions.

Meanwhile, sepiolite is a non-swelling, lightweight, porous clay with a large specific surface area. Unlike other clays, the individual particles of sepiolite have a needle-like morphology. The high surface area and porosity, as well as the unusual particle shape of this clay account for its outstanding sorption capacity and colloidal properties that make it a valuable material for a wide range of applications.

Sepiolite is a very uncommon clay because of both its peculiar characteristics and scarce occurrence.

Chemically, sepiolite is a hydrated magnesium silicate with the ideal formula $Si_{12}Mg_8O_{30}(OH)_4(OH_2)4.8H_2O$. Its structure can be described as a quincunx (an arrangement of five objects, so placed that four occupy the corners and the fifth the centre of a square or rectangle) of talc-type sheets separated by parallel channels (Figure 8). This chain-like structure produces needle-like particles instead of plate-like particles like other clays.

Sepiolite has the highest surface area of all the clay minerals, about 300 m_2/g, with a high density of silanol groups (-SiOH) which explains the marked hydrophilicity of this clay. The tiny elongated particles of sepiolite have an average length of 1µm to 2 µm, a width of 0.01 µm; and contain open channels with dimensions of 3.6 Å x 10.6 Å running along the axis of the particle.

These particles are arranged forming loosely packed and porous aggregates with an extensive capillary network which explains the high porosity of sepiolite and its light weight because of the large void space.

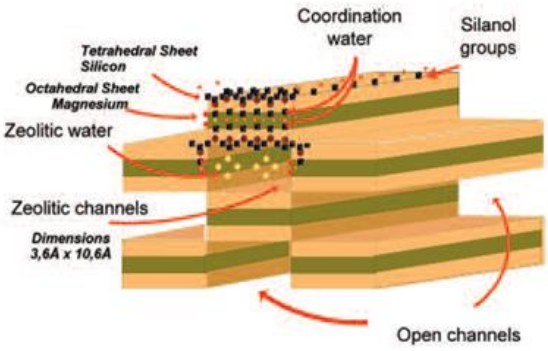

Figure 8: Sepiolite structure

The outstanding sorptive and colloidal properties of sepiolite provide specific solutions for a wide variety of industrial applications: cat and pet litters, industrial absorbents, waste treatment, carrier for chemicals, moisture control, animal feedstuffs, fertilizers, polymers and elastomers, roof panels, etc.

The use of these particles in this work is aimed to check their effectiveness as nucleating agents in PS foams for which it is necessary to have well-dispersed particles and to compare the achieved effectiveness by sepiolites with the one obtained by talc particles, the conventional nucleating agent used in the production of low density polystyrene foams.

Talc is a mineral composed by hydrated magnesium silicate with the chemical formula $H_2Mg_3(SiO_3)_4$ or $Mg_3Si_4O_{10}(OH)_2$. It has no direct origin in nature, but their formation is related to reactions between mineral species of the form:

$$3CaMg(CO_3)_2 + 4SiO_2 + H_2O \text{ ----> } Mg_3[(OH)_2Si_4O_{10}] + 3CaCO_3 + 3CO_2$$

Its laminar structure (Figure 9) is formed by two SiO_4 tetrahedral layers that are joined together by three vertices by Si-O-Si bonds, giving a distorted hexagonal ring configuration. In between these two layers is positioned an interlamellar extract formed by an octahedral layer of $Mg(OH)_6$. This creates a three-dimensional periodic structure type 2:1. Sheets are electrically neutral and are joined together by weak Van der Waals forces.

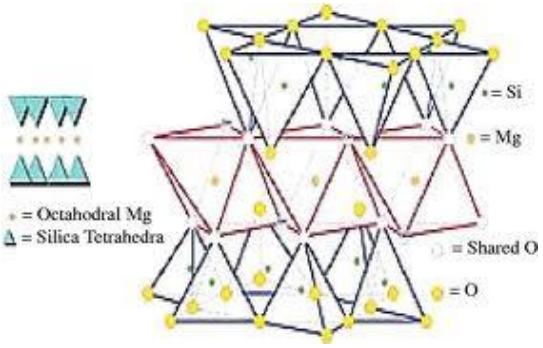

Figure 9: Talc structure

Talc has an average particle size (in the plane of the particle) of the order of microns and is presented in form of powder.

Nowadays, it is used in many industries such as paper making, paint and coatings, rubber, food, electric cable, pharmaceuticals, cosmetics, ceramics and polymers. In polymer applications talc is used as a filler or as a nucleating agent. Talc contrarily to other minerals (e.g. calcite, serpentines, micas) has proved to be particularly efficient filler on the mechanical properties and macromolecular orientation of a composite [46-48].

2.6 BLOWING AGENTS

A blowing agent can be defined as the substance that generates a cellular structure in the material [6]. The most common classification of the blowing agents is based on the mechanism by which gas is released. Taking this into account, they can be classified as chemical blowing agents and physical blowing agents [37].

-Chemical blowing agents (CBA)

They are compounds or blends of compounds that release the gas as a result of a chemical reaction [37]. In general, CBA are decomposed generating one or more gases that are used to expand the polymer. In addition, as a result of that decomposition, a certain amount of residue that remains afterwards in the material is generated [6].

Moreover, chemical blowing agents can be classified in endothermic and exothermic depending on if they absorb or release heat during their decomposition [37, 6]. Endothermic CBA absorb heat during their decomposition, while exothermic CBA release heat during their decomposition.

Azodicarbonamide is the most used exothermic chemical blowing agent. It decomposes between 200 and 220ºC producing a large amount of gas. Among the gases released, the most important ones are N_2 (around 62%), CO and NH_3 [39, 40]. Decomposition point can be reduced to temperatures around 150-160ºC by adding catalysts such as ZnO.

-Physical blowing agents

Physical blowing agents generate the gas necessary to expand the polymer by a change of state, or a change in solubility of the gas / polymer system. Generally they are low boiling liquids or gases. The most common are hydrocarbons, halogenated hydrocarbons or some inert gas such as CO_2 or N_2 [6].

When a polymer is saturated with a gas in supercritical state and it is rapidly depressurized, becomes supersaturated, so that cells nucleate and grow until the polymer vitrified or solidifies again [37, 38].

This phenomenon is used to produce microcellular foams which are characterized by having cell sizes smaller than 10µm and high cell densities [38].

2.7 SYNCHROTRON RADIATION FOR ENERGY DISPERSE X-RAY DIFFRACTION (ED-XRD)

Synchrotron radiation has become one of the most popular and powerful techniques in different fields of materials science.

It was named after its discovery in a General Electric synchrotron accelerator built in 1946 and announced in 1947 by Frank Elder, Anatole Gurewitsch, Robert Langmuir and Herb Pollock in a letter entitled "Radiation from Electrons in a Synchrotron" [41].

Synchrotron radiation emitted by accelerated electrons through wigglers and inverters is composed by a continuous spectrum of wavelengths from high energy X-ray to infrared. This radiation is very intense, concentrated and spatially coherent, ideal properties to perform a wide range of experiments to explore all kind of organic and inorganic materials using techniques such as spectroscopy, diffraction and radioscopy among others.

The first synchrotron powder-diffraction experiments based on the energy-dispersive (ED) diffraction technique were reported three decades ago [42-44]. The wide application of the ED method to problems in the field of materials science is strongly related to the increasing availability of modern 3rd generation synchrotron radiation sources.

For ED diffraction experiments with high energy synchrotron radiation, several beamlines are available today. In Europe, for example, the ID 15 and BW5-beamline at ESRF and HASYLAB, respectively, provide very high energies up to 300KeV.

This work was carried out at the materials science beamline EDDI (Energy Dispersive Diffraction) at the Berlin synchrotron storage ring BESSY. Features like a photon flux much higher than that provided by common X-ray sources or the wide energy spectrum that it uses make that system one of the most appropriated to study in-situ the foaming process of polymeric materials [45].

2.8 BIBLIOGRAPHY

[1] L.J. Gibson and M.F. Ashby. Cellular Solids: Structure and Properties. 2nd Edition, Cambridge University Press, United Kingdom, (1997)

[2] N. Mills. Polymer Foams Handbook: Engineering and Biomechanics Applications and Design Guide. 1st Edition, BH Elsevier, United Kingdom, (2007)

[3] D. Klempner and V. Sendijarevic. Handbook of Polymeric Foams and Foam Technology. 2nd Edition. Hanser Publishers, Munich, (2004)

[4] M.F. Ashby, A. G. Evans, J.W. Hutchinson, and N. A. Fleck, Metal foams: A Design Guide. Cambridge University, Engineering Department, Cambridge (1998)

[5] E. Solórzano. Espumas de Aluminio: Proceso de Espumado, Estructura Celular y Propiedades. Tesis Doctoral, Universidad de Valladolid, (2008)

[6] D. Eaves. Handbook of Polymer Foams. Rapra Technology, United Kingdom, (2004)

[7] D. Klempner and K. C. Frisch. Handbook of Polyolefin Foams and Foams Technology. Carl Hanser Verlag, Munic, (1991)

[8] A. Cunnigham and N.C. Hilyard. Phisical Behaviour of Polymeric Foams. An Overview en Low Density Cellular Plastic-Physical basis of Behaviour. Chapman and Hall (1994)

[9] M.A. Rodríguez-Pérez. Propiedades Térmicas y Mecánicas de Espumas de Poliolefinas. Tesis Doctoral, Universidad de Valladolid, (1998)

[10] R. Gendron (Ed). Thermoplastic Foam Processing. Principles and Development. CRC Press, Boca Raton-Florida, (2005)

[11] X. Cao, L. J. Lee, T. Widya, C. Macosko, *Polymer*, 46, 775–783 (2005)

[12] C. Zeng, X. Han, L. J. Lee, K. W. Koelling, D. L. Tomasko, *Advanced Materials,* 15(20), 1743-1747 (2003).

[13] S.C. Tjong, *Materials Science and Engineering*, 53, Issues 3-4, 73-197, 30 (2006)

[14] L.J. Lee, C. Zeng, X. Cao, X. Han, J. Shen, G. Xu. Polymer Nanocomposite Foams. Composites Science and Technology, 65, 2344-2636 (2005)

[15] Z. Spitalsky, D. Tasis, K. Papagelis, C. Galiotis. Progress in Polymer Science, 35, 357-401 (2010)

[16] M.C. Saha, Md.E. Kabir, S. Jeelani, *Materials Science and Engineering,* 479, 213-222 (2008)

[17] S.H. Joo, S.J. Choi, I. Oh, J. Kwak, Z. Liu, O. Terasaki, R. Ryoo, *Nature* 412, 169-172 (2001)

[18] B. Wetzela, F. Hauperta, M.Q. Zhangb, *Composites Science and Technology,* 63, 2055–2067 (2003)

[19] C.C. Ibeh, M. Bubacz. J.Cell. Plast. 44, 493-515 (2008)

[20] J.S. Colton, N.P. Suh. Polymer Engineering and Science, 27, 500-503 (1987)

[21] C. Saiz-Arroyo, J. Escudero, M.A. Rodríguez-Pérez, J.A. de Saja. Cellular Polymers, 30, 63-78 (2011)

[22] C. Saiz-Arroyo, M.A. Rodríguez-Pérez, J.I. Velasco, J.A. de Saja. Journal of Nanoparticle Research, (2013)

[23] B. Krause, H.J.P. Sijbesma, P. Munuklu, F.A. Van Der Vegt, M. Wessling, Macromolecules, 34, 8792 (2001)

[24] A.R. Sumarno, G.S. Bernardus, A.S. Ismail, Putu Teta, P. A. Proceeding of the Eight meeting on Supercritical Fluids (Chemical Reactivity and material processing in supercritical fluids); Bordeaux, 144–152 (2002)

[25] K.A. Arora, A.J. Lesser, T.J. McCarthy. Polym Eng Science, 38, 7610 (1998)

[26] S. Doroudian'i, C.B. Park, M. Kortschot. Polym Eng Sci. 38, 1205 (1998)

[27] S. Doroudian'i, C.B. Park, M. Kortschot. Polym Eng Sci. 36, 1437 (1996)

[28] H. Sun, G.S. Sur, J.E. Mark. Eur Polym J. 38, 2373 (2002)

[29] H. Sun, J.E. Mark. J Appl Polym Sci. 86, 1692 (2002)

[30] Y.K. Kwon, H.K. Bae. Korean J Chem Eng. 24, 127 (2007)

[31] C. Jo, H.E. Nagui. Cell Polym. 24, 177 (2005)

[32] D.F. Baldwin, C.B. Park, N.P. Suh. Polym Eng Sci, 36 (1996)

[33] S. Siripurapu, J.M. De Simone, S.A. Khan, R.J. Spontak. Adv Mater, 16 (2004)

[34] R. Verdejo, M. Mar Bernal, LJ. Ramsanta, FJ. Tapiador and M.A. López-Manchado, *Cellular Polymers*, 30, 45-62 (2011)

[35] Nourbakhsh, A, Ashori, A, *Journal of Applied Polymer Science*, 112, 1386-1390 (2009)

[36] Nourbakhsh, A, Ashori, A, *Journal of Applied Polymer Science*, 112, 1386-1390 (2009)

[37] D. Klempner, V. Sendijarevic. Handbook of Polymeric Foams and Foam Technology. 2nd Edition. Hanser Publishers, Munich (2004)

[38] K.T. Okamoto. Microcellular Processing. Hanser Publishers, Munich (2003)

[39] J.A. Reyes-Labarta, A. Marcilla. J. Appl. Sci. 107, 339-346 (2008)

[40] A.S. Bhatti, D. Dollimore. Thermoch. Acta, 76, 63-77 (1984)

[41] F.R. Elder, A.M. Gurewitsch, R.V. Langmuir, H.C. Pollock. Physical Review, 71, Issue 11, 829-830, (1947)

[42] L. Gerward, S. Morup, H. Topsoe, J. Appl. Phys. 47 822 (1976)

[43] B. Buras, J.S. Olsen, L. Gerward, G. Will, E. Hize, J. Appl. Cryst. 10, 431 (1977)

[44] A.M. Glazer, M. Hidaka, J. Bordas, J. Appl. Cryst. 11, 165 (1978)

[45] Ch. Genzel, I.A. Denks, J. Gibmeier, M. Klaus, G. Wagener. Nuclear Instruments and Methods in Physics Research A, 578, 23-33, (2007)

[46] L. Shucai, P.K. Jarvela, A. Jarvela. J. Appl. Polym. Sci. 71, 1641, 1649 (1999)

[47] F. Rybnikar. Eur. Polym. J. 27, 549 (1991)

[48] B. Pukansky, K. Belina, A. Rockenbauer, F.H.J. Maurer. Composites. 25, 205 (1994)

3. STATE OF ART

The two key topic that have been reviewed in this section are dispersion/ exfoliation of nanoclays and cellular nanocomposites based on PE and PS.

3.1 DISPERSION/ EXFOLIATION OF NANOCLAYS

There are four basic structures for polymer/clay mixtures: conventional clay-filled composites with micron-sized aggregates of clay particles, nanocomposites with intercalated clay, exfoliated nanoparticles with locally ordered structure and exfoliated nanocomposites with disordered structure. The objective of clay/polymer nanocomposites technology is to achieve the best dispersion and distribution in a polymer matrix. Actually three main methods for achieving it can be found in the literature [1, 2].

1. Polymerization in the presence of organoclay.
2. Melt compounding of a polymer with a suitable organoclay complex.
3. Other methods as ultrasonic exfoliating of organoclays in a low molecular weight polar liquid or co-precipitation [3-5].

Numerous examples on nanocomposites based on very different polymers and produced by any of the three previously mentioned routes can be found in the literature.

Regarding to polyethylene (PE), the first two methods are the most extended ones. The polymerization in the presence of organoclays consists of the intercalation of the clay with a compound that subsequently enters the polymerization reaction. Jin et al reported full exfoliation of polyethylene/montmorillonite system prepared by Ziegler-Natta polymerization of ethylene in the presence of organoclay [6]. Although after the polymerization the degree of exfoliation was high, a partial reaggregation of MMT platelets resulted after processing by compression molding. Alexandre et al. polymerized polyethylene in the presence of either montomorillonite or hectorite [7]. Clay exfoliation in the reaction products was confirmed by XRD and TEM but the tensile properties of the resulting nanocomposites were poor and essentially independent of the nature and content of the silicate. This evidences that the previous systems are thermodynamically unstable and the strong-solid interaction between platelets drives the phase separation.

Melt blending overcomes these difficulties and industrially is the preferred method for preparing clay/polymer nanocomposites with thermoplastic polymeric matrices. Typically, the polymer is melted and combined with the desired amount of the intercalated clay in an extruder, internal mixer or continuous mixer. Wang et al. produced polyethylene/clay nanocomposites by melt blending and determine their flammable properties [8]. The heat release rate is reduced by 32% for the nanocomposites in comparison to the raw polyethylene. The microstructure and mechanical properties of PE/clay melt blended nanocomposites were determined by Liang and co-workers [9]. Thermodynamically the melt blended nanocomposites are stable but the achievement of fully exfoliated morphologies is not easy.

Commonly the nanocomposites exhibit the more attainable intercalated/exfoliated structures, with higher or lower degrees of exfoliation in each case.

With respect to polystyrene, polymerization in the presence of organoclay is the most extended method although some works in which the melt compound method is used can be found in the literature. Guoyun et al. prepared polystyrene/sepiolite composites by in-situ intercalation polymerization [10]. By means of X-ray diffraction, Fourier transform infrared (FTIR), scanning electron microscopy (SEM) and transmission electron microscopy (TEM) they demonstrated that sepiolite was partially dispersed. Zhiping et al. synthesized polystyrene/organo-sepiolite composites by suspension polymerization and studied the thermal properties of the compound [11]. Thermal stability of the system polymer/nanoclays was higher when compared with the pure polymer. PP/PS-sepiolite nanocomposites were fabricated by Jing et al [12]. Firstly, in-situ emulsion polymerization was used to prepare the PS/sepiolite. Then the PP/PS sepiolite nanocomposites were obtained via melt-intercalation method. A uniform nanometer dispersion of the sepiolites in the polystyrene matrix was shown in SEM images. Using a Brabender Plasticorder, Morales et al. melt blended PVF_2/PMMA and PVF_2/PS with sepiolites in order to study the effect of the filler on the morphology and thermal properties of the systems [13]. As a result, they showed that the addition of the sepiolites did not affect either the compatibility or the thermal behavior of the PVF_2/PMMA system, whereas a better compatibilization is achieved for the blend PFV_2/PS under certain conditions.

In this work, a twin-screw extruder will be used to melt and blend the polymer with the filler both for the PE/ MMT system as for the PS/Sepiolites one.

3.2 CELLULAR POLYETHYLENE/ POLYSTYRENE NANOCOMPOSITES

The number of works dealing with the production and characterization of polymeric nanocomposites foams has rapidly increased in the last few years. The efforts have been focused both on thermoplastic (amorphous and semi-crystalline) and thermoset polymers. The infused nanoparticles have been also very diverse, from carbon nanotubes or nanoclays (mainly montmorillonite) to carbon nanofibers or silica particles [14-20]. Although both physical and chemical blowing agents have been used, the vast majority of the published studies deal with the former ones.

Information regarding foamed polyethylene/nanoparticles systems is scarce though some examples can be found. The semi-crystalline character of polyethylene adds a severe difficulty to the foaming using physical blowing agents. Lee et al. investigate the effect of clay particles on the cell morphology of HDPE/clay nanocomposites foams produced using a batch foaming process [21]. They proved that in comparison with neat HDPE, foamed nanocomposites presented finer and more uniform cellular structures. The influence of clays dispersion on the extrusion foaming by supercritical CO_2 of LDPE was also studied by Lee et al. [22]. Riahinezhad studied the correlation between rheology and morphology in blends of PE/EVA containing

clays [23], reductions in the cell sizes and increments in the cell density were found with the addition on the layered silicate nanoparticles. Finally Saiz-Arroyo et al. studied the foaming behavior of a more uncommon system of polyethylene containing nanosilicas. Two foaming routes were used for this purpose, one following the pressure quench method using CO_2 as blowing agent and another one using the improved compression molding route using azodicarbonamide [24].

Most of the works dealing with nanoclays and polystyrene are based on the use of montmorillonite (MMT). We have not found previous literature in which sepiolite had been used to modify the structure and properties of polystyrene foams. Martínez et al. analyzed the effect of organically modified layered double hydroxides (LDH) nanoparticles in polystyrene (PS), poly(styrene-co-acrylonitrile) (SAN), and poly(methyl methacrylate) (PMMA) foams produced using a high-pressure CO_2 dissolution foaming process [25]. A reduction in the average cell size and an increase in cell density were observed for all the materials with addition of LDH particles. A similar result was obtained by Ngo et al who introduced both montmorillonite and fluorohectorite to process PS nanocomposites foams using a batch foaming process [26]. Hwang et al. used organically modified montmorillonite to produce PS foams by injection molding using N_2 as blowing agent [27]. An increase in mechanical strength and cell density, an enhanced thermal stability and a reduction in the average cell size were obtained with the addition of the nanoparticles. Finally, Wee et al. studied the dispersion and rheological behavior of PS/montmorillonite nanocomposites and produced foams by gas dissolution foaming process [28]. On the one hand, owing to intercalated structure between the polymer and layered silicates, modulus and viscosity were enhanced with increasing clay content. On the other hand, the addition of nanoparticles reduced the cell size and increased the cell density.

3.3 BIBLIOGRAPHY

[1] L.A. Utracki in Clay-containing polymeric nanocomposites. Rapra Technology Limited. United Kingdom (2004)

[2] J.J. Koo in Polymer Nanocomposites. McGraw-Hill. USA (2006)

[3] E.C. Lee, D.F. Mielewski, R.J. Baird, Polym. Eng. Sci., 44 (9) 1773-1782 (2004)

[4] C. Lam, K. Lau, H. Cheung, H. Ling. Mat. Lett. 59 (11) 1369-1372 (2005)

[5] J. Li, G. Jiang, S.Y. Guo, L.J. Zhao. Plast. Rubb. Compos. 36 (7) 308-313 (2007)

[6] Y.H. Jin, H.J. Park, S.S. Im, S. Y. Kwak, S. Kwak. Macroml. Rapid. Commun. 23, 135-140 (2002)

[7] M. Alexandre, P. Dubois, T. Sun, J.M. Garces, R. Jerome. Polymer 43 2123-2132 (2002)

[8] S. Wang, Y. Hu, Q. Zhongkai, Z. Wang, Z. Chen, W. Fan. Mat Lett. 57 (18) 2675-2678 (2003)

[9] G. Liang, J. Xu, S. Bao, W. Xu. J. Appl. Polym. Sci. 91, 3971-3980 (2004)

[10] Z. Guoyun, P. Li, Y. Xiufang, L. Fuyong. New Chemical Materials. (2011)

[11] L. Zhiping, Y. Fei, H. Yanqiu, D. Shaobo, R. Roger, Y. Xinwei. (2007)

[12] G. Jing, L. Xiao-meng, Y. Guo-bao, G. Fu-cheng, L. Jia-xuan, H. Cheng-nv. Journal of Dalian Polytechnic University. (2011)

[13] E. Morales, C.R. Herrero, J.L. Acosta. Polymer Bulletin. 25, 391-396 (1991)

[14] W. Zhai, C. B. Park, m. Kontopoulou. Ind. Eng. Chem. Res. 50, 7282-7289 (2011)

[15] C. Zeng, X. Han, L.J. Lee, K.W. Koelling, D.L. Tomasko. Adv.Mater. 15, 1743-1747 (2003)

[16] Y.H. Lee, K.H. Wang, C.B. Park, M.Sain. J. App. Polym. Sci. 103, 2129-2134 (2007)

[17] S.M. Seraji, M.K.R. Aghjeh, M. Davari, M.S. Hosseini, S. Khelgati. Polym. Compos. 32, 1095-1105 (2011)

[18] M.C. Saha, M.E. Kabir, S. Jeelani. Mat. Sci. Eng. A-Struct. 479, 213-222 (2008)

[19] K. Gorem, L. Chen, L.S. Schadler, R. Ozisik. J. Supercrit. Fluid. 51, 420-427 (2010)

[20] R. Verdejo, C. Saiz-Arroyo, J. Carretero-Gonzalez, F. Barroso-Bujans, M.A. Rodriguez-Perez, M.A. Lopez-Manchado. Europ. Polym. J. 44, 2790-2797 (2008)

[21] J.A. Martínez-Díez, M.A. Rodríguez-Pérez, J.A. de Saja, L.O. Arcos y Rábago, O.A. Almanza. Journal of Cellular Plastics 37, 21-42 (2001)

[22] J.I. Velasco, M. Antunes, O. Ayyad, C. Saiz-Arroyo, M.A. Rodriguez-Pérez, F. Hidalgo, J.A. de Saja. J App. Polym. Sci. 105, 1658-1667 (2007)

[23] M. Abbasi, S.N. Khorasani, R. Baheri, J.M. Esfahani. Plym. Compos. 32, 1718-1725 (2011)

[24] Y.H. Lee, C.B. Park, K.H. Wang. J. Cell. Plast. 41, 487 (2005)

[25] B. Martínez, V. Realinho, M. Antunes, M.L. Maspoch, J.I. Velasco, Ind. Eng. Chem. Res. 50, 5239–5247 (2011)

[26] TTV. Ngo, J. Duchet-Rumeau, AK. Whittaker, JF. Gerard, Polymer, 51 3436-3444 (2010)

[27] SS Hwang, PP Hsu, JM Yeh, CH Hu, KC Chang, International Communications in Heat and Mass Transfer. 36, 799–805 (2009)

[28] D. Wee, DG. Seong, JR. Youn, Fibers and Polymers. 5, 160-169 (2004)

4. OBJECTIVES

The present study aims on the one hand to achieve a better understanding of the underlying mechanisms that induce the exfoliation of montmorillonite during the foaming process in the system PE/clays by using synchrotron radiation as it allows to in-situ monitor the exfoliation process. On the other hand, the second target of this work is to understand the role played by another type of nanoparticle (sepiolite) in the foaming process of PS. With this purpose, a detailed study of the particle dispersion level within the polymer matrix has been carried out.

Taking this into account, the work will be divided in two main parts:

1. In-situ characterization of the foaming process in PE/ MMT system: a novel technique [energy dispersive X-ray diffraction (ED-XRD)] will be used to in-situ follow the exfoliation of nanoclays during foaming in a low density polyethylene (PE 003) blended with 3 wt. % and 5 wt. % of montmorillonite-type organomodified nanoclays (Cloisite 15A). Three different blowing agents (7 wt. % azodicarbonamide, 3 wt. % hydrocerol and 4 wt. % expancel) will be used in order to study the foaming behavior. The amounts of the different blowing agents were selected according to previous experiences.

Cellular materials will be produced by free foaming in a homemade vermiculite furnace composed by three infrared lamps.

The obtained diffractograms will be analyzed to check if the foaming process induces any effect on the exfoliation process of the nanoclays.

2. Characterization of dispersion in the PS/ Sepiolite system: the dispersion of nanoparticles will be studied in solid nanocomposites of polystyrene (Edistir N2380) containing sepiolite using a theoretical model and an experimental one. Images of Scanning Electron Microscopy (SEM) with backscattered electrons of the solid nanocomposites will be used to quantify the number of particles.

Cellular materials will be produced by batch gas dissolution foaming process using CO_2 as blowing agent. Cellular structure will be analyzed by SEM.

Results from theoretical and experimental methodologies will be compared in order to study the dispersion of the sepiolite along the polymer matrix. In addition, these results will be compared with the ones obtained using SEM for the cellular structure to study the effectiveness of the nanoclays as nucleating agents.

The same procedure will be applied to the polystyrene/talc system to search for similarities or differences between both systems.

5. EXPERIMENTAL

5.1 MATERIALS AND SAMPLE PREPARATION

In-situ characterization of the foaming process in PE/ MMT system

A low density polyethylene PE003 from Repsol Alcudia with a melt flow index of 2 g/10min (measured at 190 ^{o}C and 2.16Kg), a density of 920 kg/m^3 and 110 ^{o}C of melting point was used as polymer matrix. For the nanocomposites this polymer matrix was melt blended with montmorillonite-type organomodified nanoclays Cloisite C15A from Southern Clay Products and a coupling agent, maleic anhydride grafted polyethylene Fusabond 226 DE from DuPont (1.5 g/10min, 120 ^{o}C of melting point). The blending was performed in a twin screw extruder Bühler BTSK 20/40D at 250 rpm with a die temperature of 190 ^{o}C. The proportion of coupling agent to nanoclays was maintained constant in 2:1.

In order to study the foaming behavior the previous nanocomposites were blended with three different blowing agents (7 wt.% of Azodicarbonamide, 3 wt.% of Hydrocerol and 4 wt.% of Expancel) and antioxidants Irgafos 168 (from Ciba) in a proportion of 0.08 wt.% and Irganox 1010 (from Ciba) in a proportion of 0.02 wt.% to prevent thermal oxidation of the polymer. The blending was performed in a twin screw extruder (Collin mod ZK25T). To avoid any difference in the exfoliation of the platelets, a constant shear mixing energy was imparted to all the samples. A screw speed of 50 rpm was used in all the formulations with a constant feeding speed and a temperature profile identical for all the compositions. This was varied from 105ºC in the hopper to 125ºC in the die, in steps of 5ºC. Such profile was chosen in order to avoid premature decomposition of the blowing agents during the compounding steps. The material was water cooled and pelletized.

The three blowing agents that were used are:

- *Azodicarbonamide* (Porofor ADC/M-C1 from Lanxess). An exothermic chemical foaming agent presented as a yellow powder which has an average particle size of (3.9 ± 0.6) µm and onset of decomposition around 210ºC. The main released gases are N_2 (62%), CO (35%) and NH_3 (less than 3%) [1, 2]. In the following it will be denoted as AZO.

- *Hydrocerol* (BIH 40 E from Clariant). An endothermic chemical foaming agent handle as masterbatch in form of white pellets with a 60% of active compound which has an onset of temperature decomposition of 140ºC. The main products released in the reaction of decomposition are CO_2 and H_2O [3-5]. In the following it will be denoted as HY.

- *Expancel* (950 DU 80 from AkzoNobel). Microspheres with a particle size comprised between 18-24µm, a density ≤ 12kg/m^3 (once expanded) that are characterized by having a dissolved gas, typically a hydrocarbon, inside of them. The onset of expansion

is about 140 ºC. Unlike the other two blowing agents mentioned above where once the temperature of decomposition is reached the gas is released, in this case when the activation temperature is reached the microspheres start to expand maintaining the gas confined within [6-8]. In the following it will be denoted as EXP.

Prior to the foaming, the formulations containing the different blowing agents were compression molded into precursors of 10 mm x 10 mm and 4 mm thickness using a two-hot plates press. In all the formulations the temperature of the press was fixed at 125ºC (lower than the decomposition point of all the used blowing agents). The material is first molten without pressure for 15 minutes, then it is pressed under a constant pressure of 2.18 MPa for another 15 minutes and finally it is cooled down under the same pressure. These molded precursors were used later for foaming.

Two different clay contents were used, 3 wt.% and 5 wt.%. Two different foaming temperatures were used also for all the samples, 185ºC and 190ºC. The compositions and nomenclature are summarized in Table 1.

Sample	Matrix/parts	Coupling agent/parts	Nanoclays /parts	wt.% Blowing Agent	Temperature / ºC
3% Nanoclays_AZO_185	91	6	3	7	185
3% Nanoclays_AZO_190	91	6	3	7	190
5% Nanoclays_AZO_185	85	10	5	7	185
5% Nanoclays_AZO_190	85	10	5	7	190
5% Nanoclays_HY_185	85	10	5	3	185
5% Nanoclays_HY_190	85	10	5	3	190
5% Nanoclays_EXP_185	85	10	5	4	185
5% Nanoclays_EXP_190	85	10	5	4	190

Table 1: Proportion of components for the different kind of samples and foaming temperature

Foaming was conducted using a free foaming process. Precursors were placed inside a homemade vermiculite furnace composed by three infrared ceramic heaters placed one on the top and the other two at both lateral sides and by a thermocouple that is introduced in the precursor with the aim of controlling the temperature of the sample. The temperature was increased from 30 up to the foaming temperatures 185 or 190 ºC at about 10K/min and held there for an isothermal step. After 600 s, the lamps were turned off and cooling took place.

Characterization of dispersion in the PS/ Sepiolite system

Three different types of sepiolite particles were tested. All of them were provided by Tolsa, S.A (Spain). First one corresponds to a non-organically modified sepiolite (labelled as UNV-1). Moreover, two surface modified sepiolites with a quaternary ammonium salt (UNV-2) and silane (UNV-3) were also tested. Non modified sepiolite (UNV-1) was obtained using a wet milling processing to defibrillate the bundles of sepiolite up to single particles and dried to remove the water content below 2 wt.%. This sample is composed by individual sepiolite needles with an average particle length ranging between 1 µm and 2 µm and a diameter in the nanometer range (ca. 20-30 nm). Surface modification of needle-like sepiolite particles was carried out from UNV-1 in the form of aqueous gels according to the procedure described in a previous work [9]. In contrast with modifications in organic solvents, reactions in water make possible to modify the surface of individual sepiolite particles and produce a continuous coating of the sepiolite surface. Modifications in aqueous gel were carried out by dispersing a defibrillated sepiolite (UNV-1) in water (4 wt%) and adding the quaternary ammonium salt (UNV-2) or silane (UNV-3) by means of a high shear mixer during 15 min. The mechanical mixing at high shear rate and the sepiolite concentration in water produced enough friction to obtain individually dispersed surface modified fibers (Figure 10). After the modification in wet medium, samples were filtered, milled and dried at 120ºC.

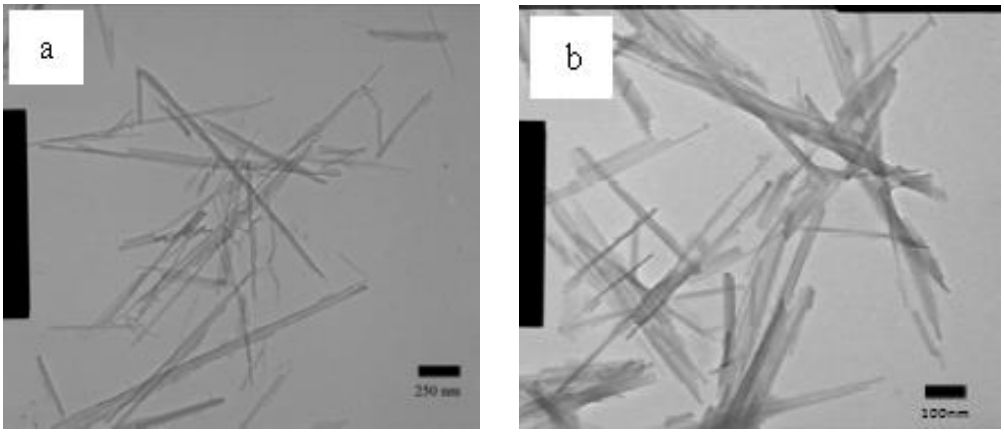

Figure 10: Transmission Electron Microscopy of non-modified (a) and modified sepiolite (b)

Talc 10M2 from Luzenac (average particle size of 3 microns) was also used as nucleating agent. As polymer matrix a conventional PS for foams applications (Edistir N2380) was used.

Table 2 shows the different formulations that were produced for the study. Pure PS, and PS+1 wt.% talc were used as reference materials. In addition to this, PS containing 1% of each type of sepiolite was also produced. Finally, materials with different amounts of the non-treated sepiolite (UNV-1) between 0.25 wt.% and 5 wt.% were produced.

All the used fillers were dried prior to compounding. The formulations were produced using a twin-screw extruder (Collin ZK 25T) with a temperature profile between 175 and 190°C. Using the previous formulations, solid precursors (80x20x2mm^3) were produced by injection molding (BabyPlast injection molding machine).

Sample	Type of Filler	Content (wt. %)
Pure PS	None	0
PS + 1% Talc	Talc	1
PS + 1% UNV-1	Non-treated Sepiolite	1
PS + 1% UNV-2	Sepiolite treated with a quaternary ammonium salt	1
PS + 1% UNV-3	Sepiolite treated with a silane	1
PS + 0.25% UNV-1	Non-treated Sepiolite	0.25
PS + 0.5% UNV-1	Non-treated Sepiolite	0.5
PS + 3% UNV-1	Non-treated Sepiolite	3
PS + 5% UNV-1	Non-treated Sepiolite	5

Table2: Formulations of the produced materials

Foaming was conducted using the batch gas dissolution foaming process. Saturation of the precursors was performed at 60°C using CO_2 at 80 bars. A time of 24 hours was enough to obtain fully saturated specimens. After a rapid depressurization drop precursors were quickly transferred to a furnace. Foaming was carried out in a pre-heated furnace at a temperature of 120°C, the materials were placed inside the furnace for three minutes. After this time they were cooled down in water.

Solid samples (Pure PS, PS +1% Talc, PS +1% UNV-1, PS +1% UNV-2 and PS +1% UNV-3) for rheological studies were prepared by compression molding using a two-hot plates press. Samples with 150 mm in diameter and 0.5mm thickness were fabricated at a fixed temperature of 145 °C for all the formulations. The material was first molten without pressure for 10 minutes, then it was pressed under a constant pressure of 2.18 MPa for another 15 minutes and finally it was cooled down under the same pressure. These molded specimens were then cut into samples of 10mm x 20mm x 0.5mm.

5.2 CHARACTERIZATION OF SOLID NANOCOMPOSITES

In-situ characterization of the foaming process in PE/ MMT system

The ex-situ dispersion and exfoliation of nanoclays were studied using X-Ray diffraction (XRD) and transmission electron microscopy (TEM). XRD diffractograms were determined between 1° and 10° by steps of 0.005° by means of a Philips PW 1050/71 using the Cu Kα line. The transmission electron microscope used was a Tesla BS 512 with a YAG camera incorporated. Several images from different areas were analyzed to obtain representative conclusions.

Characterization of dispersion in the PS/ Sepiolite system

Solid densities were determined by water-displacement method, based on Archimedes' principle using the density determination kit for the AT261 Mettler-Toledo balance. At least three measurements were carried out for each sample produced.

The possible modification of the rheological behavior by the addition of nanoparticles was studied by means of an AR2000EX TA Instruments rheometer with an extensional fixture at a temperature of 120°C (coinciding with the foaming temperature used as explained above) and at a strain rate of $1s^{-1}$.

In order to analyze sepiolite dispersion in solid nanocomposites their morphology was studied using a scanning electron microscope (SEM) with backscattered electrons (QUANTA 200F model). In the case of talc, the dispersion in solid materials was studied by means of scanning electron microscopy (JEOL JSM-820 microscope). In all cases, solid precursors were frozen in liquid nitrogen and fractured in the perpendicular direction to the injection in order to assure that the microstructure remained intact.

Particle size was measured using an image processing tool based on the software ImageJ [10].

The study of the dispersion of the nanoparticles in the solid nanocomposites was carried out by using both a theoretical model and an experimental methodology.

The theoretical model states that if it is assumed a complete dispersion of the filler, the number of particles per unit volume can be calculated using the following equation [11]:

$$\frac{nucleants}{cm^3} = \frac{w_p \rho_c}{\rho_p V_p} \qquad \text{Eq. 4}$$

where w_p is the weight fraction of the particle in the composite, ρ_p and ρ_c are the density of the particle and the polymer composite respectively, and V_p is the volume of the individual particle.

In the experimental methodology, the SEM micrographs (with and without backscattered electrons) are used to quantify the real number of particle aggregates per unit surface. By raising the obtained value to the power of 3/2, it is possible to estimate the real number of aggregates per unit volume.

To assess the difference between the two models, a new parameter called *Agglomeration Ratio* is defined. *Agglomeration Ratio* is defined as the ratio between the theoretical number of particles per unit volume divided by the real number of particles (aggregates) present in the sample (Equation 5). This parameter measures the average number of particles per agglomerate.

$$Agglomeration\ Ratio = \frac{Nºnucleants/cm^3(theoretical)}{Nºnucleants/cm^3(real)} \qquad \text{Eq. 5}$$

Another important parameter is the so called *Nucleation Efficiency*. This parameter quantifies the effectiveness of the particles as nucleating agents and can be defined as the ratio between the measured cell density and the potential nucleation density of the filler (Equation 6). Using both theoretical and experimental values of particles per unit volume it is possible to calculate both a theoretical and an experimental value of *Nucleation Efficiency*.

$$Nucleation\ Efficiency = \frac{Measured\ cell\ density}{Potential\ nucleation\ density\ of\ the\ filler} \qquad \text{Eq. 6}$$

5.3 CHARACTERIZATION OF CELLULAR NANOCOMPOSITES

In-situ characterization of the foaming process in PE/ MMT system

The exfoliation of nanoclays during foaming as well as the molten and crystallization behavior of PE together with the decomposition process of the blowing agent was followed in-situ by ED-XRD at the EDDI experimental station hosted at the BESSY II synchrotron light source of the Helmholtz Centre Berlin. Samples were illuminated by a white X-ray beam of 2×1 mm^2 (height $\times$ width) cross-section. Peaks of intensity were detected at particular energies, E_{hkl}, in transmission geometry at the angle 2θ = 1.7° for the nanoclays and at 2θ = 6° for the PE and the blowing agent by a Ge multichannel analysing detector, since the diffracted photon energies obey Bragg's law, which reads in its energy-dispersive form as $E_{hkl} = hc/2d_{hkl}\sin\theta$, where h is Planck's constant and c the speed of light (see reference [12] for a detail description of EDDI). A self-designed X-ray transparent furnace equipped with infrared lamps and Kapton windows was mounted on a positioning table attached to the goniometer (see Figure 10). The sample size was 20×10×4 mm^3. The 10 mm side was placed parallel to the beam direction and the 4 mm side indicates the compaction direction. A thermocouple was inserted into the sample parallel to the 20 mm side and beside the beam path for recording and controlling the temperature program using a CAL3300 controller and a self-develop program that runs under LabView. The temperature was increased from 30 up to the foaming temperatures 185 or 190 °C at about 10 K·min-1 and held there for an isothermal step. After 600 s, the lamps were turned off and cooling took place. ED-XRD data acquisition and positioning table were computer controlled by the software package Spec [13]. Acquisition started when the sample temperature was 100 °C on heating. The counting time per spectrum was 30 s, after which a lateral sample displacement of 1 mm was programmed in order to detect each time diffracted

photon-energies from a volume which was previously not irradiated by the X-rays. Complementary spectra were also acquired for 30 s at ambient temperature, before heating and after cooling.

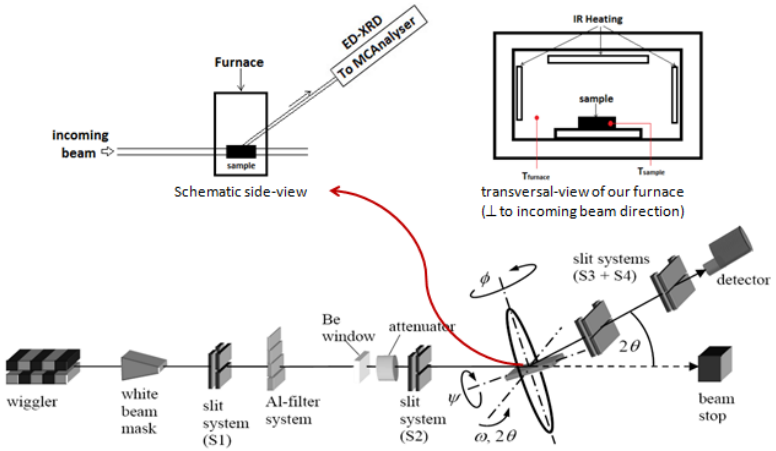

Figure 11: Schematic layout of the main beamline components and furnace used for the foaming tests.

In order to study the catalytic effect produced by nanoclays over the azodicarbonamide, a thermogravimetric analysis in N_2 atmosphere was performed using a Mettler TGA/SDTA 851e with a temperature profile identical to the one used for foaming: from 50 to 185°C at 15°C/min, isotherm at 185°C during 3 minutes and from 185 to 50°C at -6°C/min.

Characterization of dispersion in the PS/ Sepiolite system

Foam densities were determined by water-displacement method, based on Archimedes' principle using the density determination kit for the AT261 Mettler-Toledo balance. At least three measurements were carried out for each sample.

Open cell content of foamed materials was determined according with ASTM Standard D6226-10 using a gas pycnometer, model AccuPyc II 1340.

Cellular structure of the whole collection of foams was analyzed using Scanning Electron Microscopy (SEM). In order to not distort their microstructure, samples were frozen in liquid nitrogen and afterwards fractured. Surface fracture was made conductive by sputtering deposition of a thin layer of gold and observed using a JEOL JSM-820 Scanning Electron Microscope.

Cell density and cell size were measured using an image processing tool based on the software ImageJ [10]. This software provides the cell size distribution, the average cell size, the cell anisotropy ratio distribution, the average cell anisotropy ratio, the cell density N_v (cells/cm^3) and the nucleation density N_o (nucleation points/cm^3), that can be calculated from N_v according to equation 7 [14]:

$$N_0 = \frac{N_v}{1-V_f} \qquad \text{Eq. 7}$$

where V_f is the volume fraction of voids.

Thermal conductivity was characterized using the Transient Plane Source (TPS) technique. In the TPS method, a round and plane heat source is used. It behaves as a transient plane source working simultaneously as a temperature sensor. The TPS element is located between two samples with both sensor faces in contact with the two samples surfaces. Samples were polished to obtain homogeneous surfaces to ensure an appropriate contact with the sensor faces. This technique has been used previously on this kind of materials with good results [15, 16].

5.4 BIBLIOGRAPHY

[1] J.A. Reyes-Labarta, A. Marcilla. J. Appl. Sci. 107, 339-346 (2008)

[2] A.S. Bhatti, D. Dollimore. Thermoch. Acta, 76, 63-77 (1984)

[3] M.E. Gomes, J.S. Godinho, D. Tchalamov, A.M. Cunha, R.L. Reis. J. Appl. Med. Polym. 6, 75-80 (2002)

[4] X. Qin, M.R. Thompson, A.N. Hrymak. Polym. Eng. Sci. 47. 522-529 (2007)

[5] A.K. Bledzki, O. Faruk, J. Cell. Plast. 41. 539-550 (2005)

[6] H. Andersson, P. Griss, G. Stemme. Sens. Act. 84, 290-295 (2002)

[7] J. Yao, M.R. Barzegari, D. Rodrigue. Cell. Polym 20. 5-19 (2010)

[8] T. Ohji, T. Sekino, K. Niihara. Key Eng. Mat. 317-318. 899-904 (2006)

[9] N. García, J. Guzmán, E. Benito, A. Esteban-Cubillo, E. Aguilar, J. Santarén, P. Tiemblo. Langmuir, 27, 3952-3959 (2011)

[10] J. Pinto, E. Solórzano, M. A. Rodriguez-Perez, J. A. de Saja. Journal of Cellular Plastics (in press)

[11] W. Zhai, J. Yu, L. Wu, W. Ma, J. He. Polymer 47, 7580-7859 (2006)

[12] Ch. Genzel, I.A. Denks, J. Gibmeir, M. Klaus, G. Wagener. Nuclear Instruments and Methods in Physics Research A, 578, 23-33 (2007)

[13] J.H. Koo in Polymer Nanocomposites. McGraw-Hill. USA (2006)

[14] V. Kumar, N. P. Suh. Polymer. Eng. Sci., 30, 1323 (1990)

[15] O. Almanza, M.A. Rodríguez-Pérez, J.A. de Saja. J. Polymer Sc. (B), 42, 1226-1234 (2004)

[16] J.A. Reglero-Ruiz, C. Saiz-Arroyo, M. Dumon, M.A. Rodríguez-Pérez, L. González. Polym. Int., 60, 146 (2010)

6. RESULTS AND DISCUSSIONS

6.1 IN-SITU CHARACTERIZATION OF THE FOAMING PROCESS IN PE/ MMT SYSTEM

Characterization of the solid nanocomposites

An ex-situ X-Ray diffraction (XRD) study of the nanocomposites was performed prior to the in-situ foaming in the synchrotron beamline with the aim of knowing the initial interlamellar space of the nanoclays before foaming and comparing the results with the corresponding ones obtained later in the synchrotron. Figure 12 shows the XDR pattern of the nanocomposites (with a 3wt. % and 5wt. % of AZO) compared with the XRD pattern of the nanoclays as received. From this figure, the Bragg´s Law yields a separation between platelets of 2.45nm for the organomodified nanoclays as received and this separation is increased up to 3.27nm for the nanocomposites, always taking the maximum of the peaks for the calculation. This suggests that the use of a compatibilising agent and the choice of appropriate extrusion parameters have promoted some intercalation degree although there are still agglomerates present in the polymer matrix. An intercalated/ exfoliated structure is hypothesized for the nanocomposites.

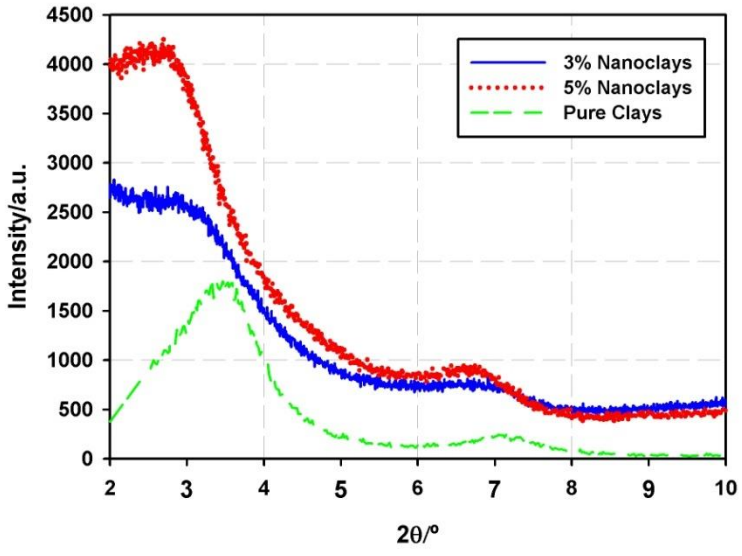

Figure 12: Ex- situ XRD pattern for the pure clays and for the melt blended nanocomposites.

Transmission electron microscopy (TEM) images confirm this structure. Figure 13 shows two micrographs for the 5% nanoclays samples. On Figure 13a) individual well exfoliated and dispersed platelets can be distinguished all along the micrograph but in some areas (Figure 13b)) still some agglomerates of platelets that have not suffered a complete exfoliation can be observed.

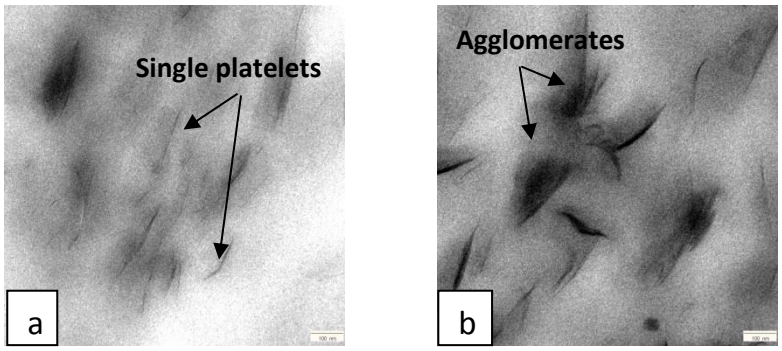

Figure 13: TEM images. Left: single platelets can be distinguished with a good dispersion. Right: still some large stacks are present.

On the other hand, the diffraction pattern obtained for the 5wt. % nanoclays filled samples (precursors before foaming) with the different blowing agents and for the nanocomposites without any blowing agent is presented in Figure 14. Since the processing conditions of all the composites have been the same the differences found in the aggregation state of the clays can be only attributed to the different nature of the blowing agents employed.

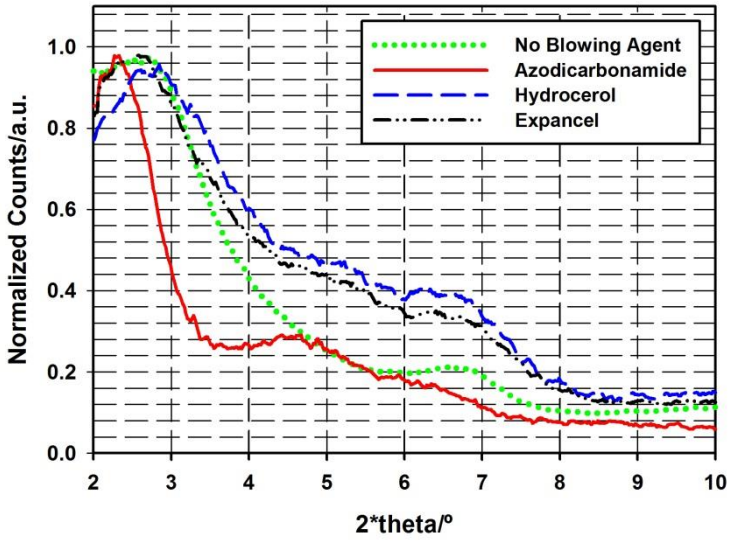

Figure 14: Ex- situ XRD pattern for the solid precursors containing 5wt. % of blowing agent and for the solid matrix without blowing agent.

In the samples that combine azodicarbonamide with nanoclays the main diffraction peak is shifted to lower angles compared to the rest of the samples. Indeed, in the samples blended with hydrocerol or expancel, the peak coincides with the one of the samples without foaming agent. This suggests that there exists some kind of chemical interaction between the azodicarbonamide and the nanoclays that promotes some degree of exfoliation during blending. On the contrary, the state of aggregation of the nanocomposites remains unaltered after blending with hydrocerol or expancel. This interesting result observed ex-situ will be later supported by the in-situ data.

Characterization of foamed nanocomposites

Effects related to the nature of the blowing agent

Solid nanocomposites filled with 5wt. % of nanoclays were foamed at two different temperatures (185ºC and 190ºC) using three different blowing agents.

The results provided by the EDDI beamline are given in the form represented in Figure 15. This figure shows the phase transformation sequence undergone by a sample containing azodicarbonamide and foamed at 185ºC. The sequence is represented in a density plot of diffracted intensities dispersed in energies vs. time. Several important points can be highlighted from this figure. Firstly, it can be observed how PE signal disappears from t = 220 seconds due to the polymer melting. At t ≈ 1500s, PE signal reappears due to the solidification of the polymer. The signal from the chemical blowing agent it is also observed, showing that as time increases, the peak is shifted to lower energies meaning that azodicarbonamide is decomposing. These effects can be better appreciated in Figure 16 where an amplification of Figure 15 has been plotted.

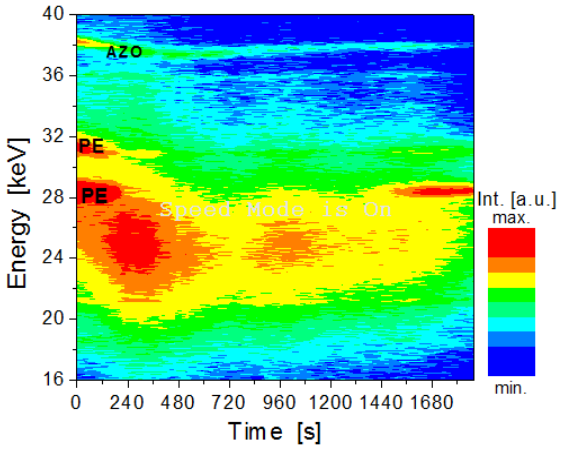

Figure 15: Phase transformation sequence for a sample containing AZO and foamed at 185ºC.

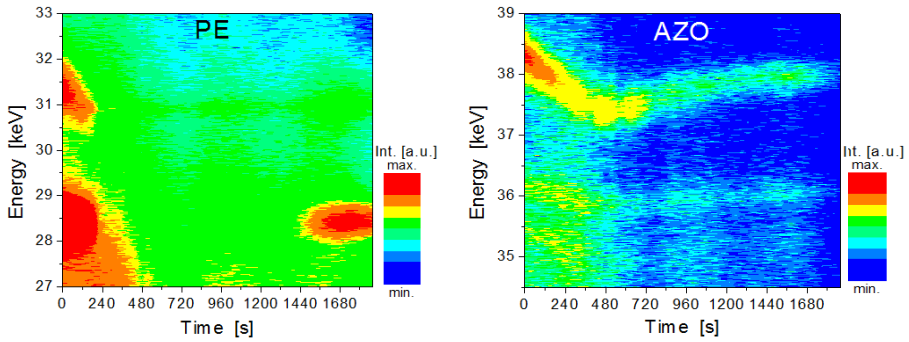

Figure 16: Amplification of the phase transformation sequence both for the PE signal and for the AZO one.

In order to detect the signal from the nanoclays, the angle was shifted to lower values. An identical plot to the one obtained for PE and AZO (Figure 15) was acquired for the MMT (not showed here). From this kind of plots, each individual in-situ diffractogram can be obtained. Figure 17 shows the diffractograms obtained at different instants for a sample containing

azodicarbonamide and foamed at 185ºC. For a better visualization, only the first and the last spectrum are shown in Figure 18. It can be observed how as time increases, the characteristic peak of the nanoclays (see the arrows) shifts to lower angles which indicates that the interlamellar distance increases.

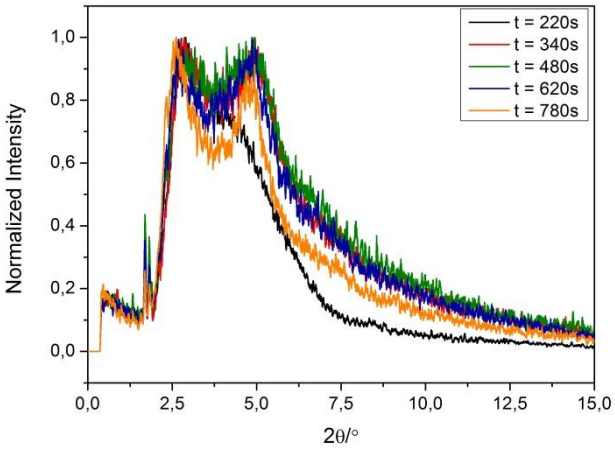

Figure 17: In-situ diffractograms obtained at different times for a sample containing AZO at 185ºC.

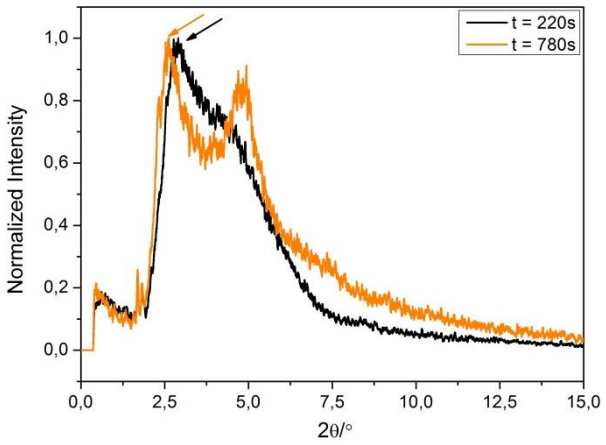

Figure 18: First and last in-situ diffractograms acquired during the foaming process.

Such interlamellar distance determined from the in-situ diffractograms during foaming is represented in Figure 19 as a function of the foaming time. The sample temperature profile is also included. As it was mentioned above (see section 5.3), prior to the continuous acquisition of diffractograms, two complementary spectra were acquired at ambient temperature before heating and after cooling. These spectra correspond to time points equal to 0 and equal to 4500 seconds respectively.

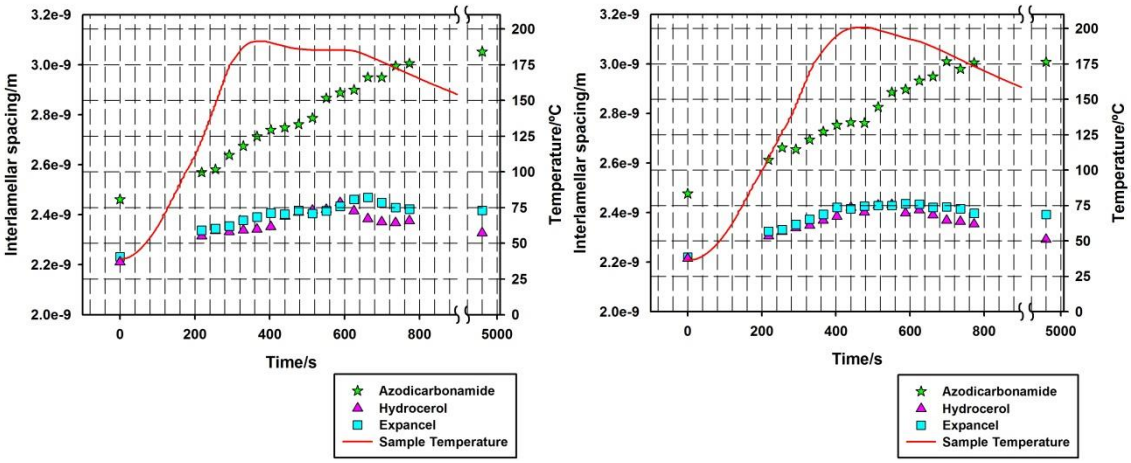

Figure 19: In-situ characterization of the evolution of the interlamellar distance as a function of foaming time.

In the initial stage of the curves, at t=0s, the separation between platelets in the samples blended with azodicarbonamide is 10% higher than the one in samples blended with hydrocerol or expancel. This behavior follows the same trend found ex-situ and mentioned above (Figure 14). Azodicarbonamide seems to promote an increase in the interlamellar distance in MMT particles during blending.

Around t = 200s the interlamellar distance is 5% higher than the initial platelets separation (t=0 seconds). This behavior is due to the increased mobility of the polymer molecular chains that have been thermally activated (the point t = 200s corresponds to a temperature of 100ºC). This increment, attributed to the thermal movement of the polymer chains, is independently of the type of blowing agent used and for all of them reaches a value near 5%.

In the samples containing azodicarbonamide, from 540 to 560 seconds the rate of increment in the interlamellar distance is much more pronounced. At that time the sample temperature coincides with the decomposition temperature of the blowing agent. The foaming begins and therefore the interlamellar spacing is increased stronger than previously. This effect is not observed with hydrocerol or expancel since the decomposition temperature window is broader. In any case, it can be concluded that the foaming process also helps to increase the exfoliation of the clays regardless of the different foaming mechanisms involved. In the case of expancel, the gas is always confined within the microspheres, so the increment in the exfoliation is attributed to the separation suffered by the polymer chains chemically bonded to the nanoclays platelets during the expansion of the polymer. The nature of the gas released or the releasing of gas itself do not influence the exfoliation during foaming.

The expansion ratios achieved during the experiments are shown in Table 3. The maximum expansion ratio achievable using expancel and hydrocerol are lower than the one reached with azodicarbonamide. This is the reason why lower increments in interlamellar distance are later found for the samples containing hydrocerol and expancel in comparison with the azodicarbonamide ones. Therefore, a direct relationship between expansion ratio and degree of exfoliation is found. In addition, for the hydrocerol an expancel, the interlamellar distance reaches a maximum and then decays to a lower value as the foam collapses and solidifies. On the contrary, with azodicarbonamide, the collapse and solidification of the foam do not seem

to have any influence on the interlamellar distance reached, it is maintained constant. So it is hypothesized that the proposed chemical interaction between nanoclays and azodicarbonamide also helps to retain the maximum separation achieved between platelets. Since hydrocerol and expancel do not show any interaction with the layered silicates, the foam collapse and solidification produce also some collapse on the lamellar structure.

Sample	Density / (Kg/m^3)
5% Nanoclays_AZO_185	250.3
5% Nanoclays_HY_185	648.0
5% Nanoclays_EXP_185	609.5
5% Nanoclays_AZO_190	237.8
5% Nanoclays_HY_190	639.8
5% Nanoclays_EXP_190	616.8

Table 3: Final densities achieved with the different blowing agents at 185ºC and 190ºC.

Effects related to the amount of nanoclays

In this case, two different percentages of nanoclays were analyzed fixing the kind and amount of blowing agent. The final densities achieved for the different samples are shown in Table 4. The higher the percentage of nanoclays, the higher is the degree of expansion achieved. Several reasons lie behind this. The first one is related to the catalytic effect of the nanoclays over the azodicarbonamide. This effect can be demonstrated by thermogravimetric analysis as can be seen in Figure 20. “Blank for 3%” and “Blank for 5%” are samples that maintained the ratio coupling agent/ polymer matrix as in the samples with clays but without them. The weight loss measured by thermogravimetry is due to the decomposition of the azodicarbonamide, therefore to the gas released. As can be deduced from Figure 20, a higher amount of nanoclays implies a higher amount of gas released and therefore higher expansion ratios can be achieved. Not only the amount of gas released is higher in the samples with clays but the decomposition of the azodicarbonamide begins earlier in these samples. In addition, nanoclays can act as a gas barrier limiting the gas escape and increasing the amount of gas available during the foam expansion.

Sample	Density / (Kg/m^3)
3% Nanoclays_AZO_185	324.2
5% Nanoclays_AZO_185	250.3
3% Nanoclays_AZO_190	313.1
5% Nanoclays_AZO_190	237.8

Table 4: Final densities achieved in samples with the different amount of nanoclays.

In any case the samples containing 5wt. % of nanoclays reach higher expansions. Moreover, a direct correlation between increment in interlamellar distance and expansion ratio can be established again in this case as can be seen in Figure 21. These graphs were obtained in the same way to that explained in the previous section.

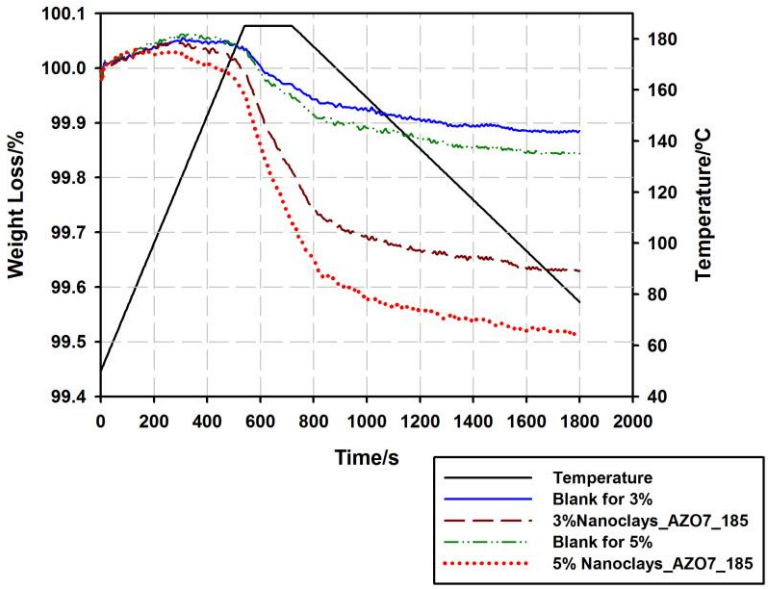

Figure 20: Thermogravimetric analysis of the samples containing different amounts of nanoclays and its corresponding blanks.

The increment in interlamellar distance attributed to the thermally activated mobility of the polymer molecular chains is observed again independently of the nanoclays addition.

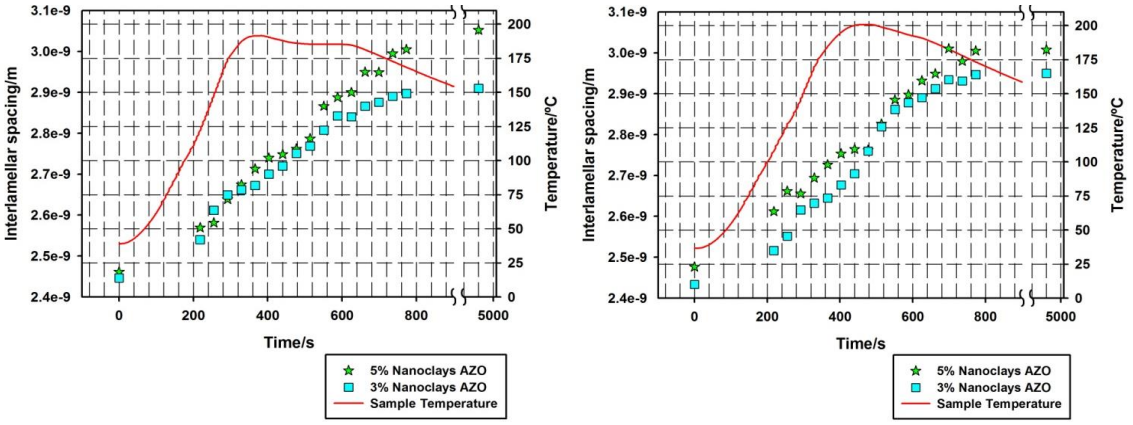

Figure 21: Evolution of the interlamellar distance during foaming in samples containing different additions of nanoparticles.

6.2 CHARACTERIZATION OF DISPERSION IN THE PS/ SEPIOLITE SYSTEM

Density

Solid injected nanocomposites filled with 1wt. % of each type of sepiolite and with 0.25 -5 wt. % of non-treated sepiolite (UNV-1) and the reference materials (Pure PS and PS+1wt. % talc) were foamed by batch gas dissolution process. CO_2 was used as physical blowing agent.

As it can be inferred from Table 5, density of the foams is affected by the addition of nanoclays. There is an increase of density which is probably due to the higher viscosity of the polymer containing the high surface area nanoparticles.

Cellular Structure

Figure 22 shows the cellular structure of the samples containing 1wt. % of the different particles, i.e. talc and the different types of sepiolites (UNV-1, UNV-2 and UNV-3) as well as the pure polystyrene. It is clearly observed a significant reduction of the cell size with respect to the reference systems due to the addition of the sepiolites. These differences can be better appreciated in Figure 23 and Table 5 where some of the main characteristics of the foams are summarized.

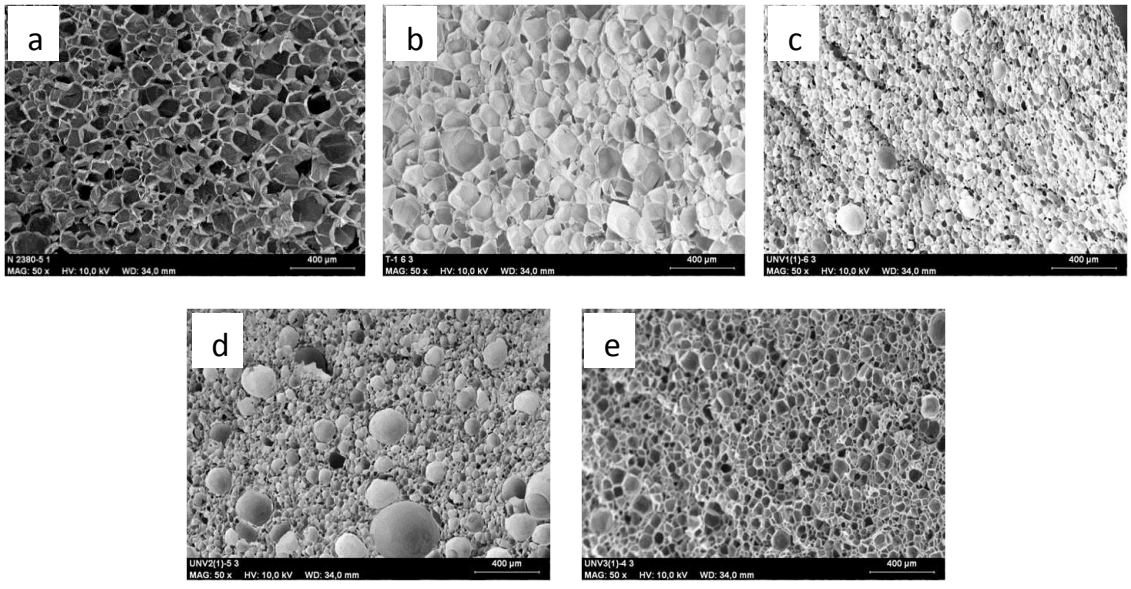

Figure 22: Micrographs showing the cellular structure of samples a) Pure PS, b) 1% Talc, c) 1% UNV-1, d) 1% UNV-2, e) 1% UNV-3.

The reduction of the cell size is significant, from around 200 microns for the pure PS or 86 microns for the sample containing talc to around 37 microns for samples containing 1% sepiolites. These changes are reflected in an increase of the cell density. The three types of sepiolite have a similar effect, giving very similar cell densities. Moreover, the standard deviation of the cell size measurements, which is related to the cellular structure homogeneity, is reduced when the nanoparticles are used. Finally, it is also observed that a

bimodal cell size distribution appears for samples containing the sepiolite modified with quaternary ammonium salts (UNV-2).

The increase of cell density in two orders of magnitude respect to the pure polystyrene or in one order of magnitude respect to the system containing talc seems to be due to the higher nucleation activity of the sepiolites in comparison with talc. For a similar content of filler, the smaller the particle size, the higher are the number of nucleation sites for the cells, and therefore higher cell density.

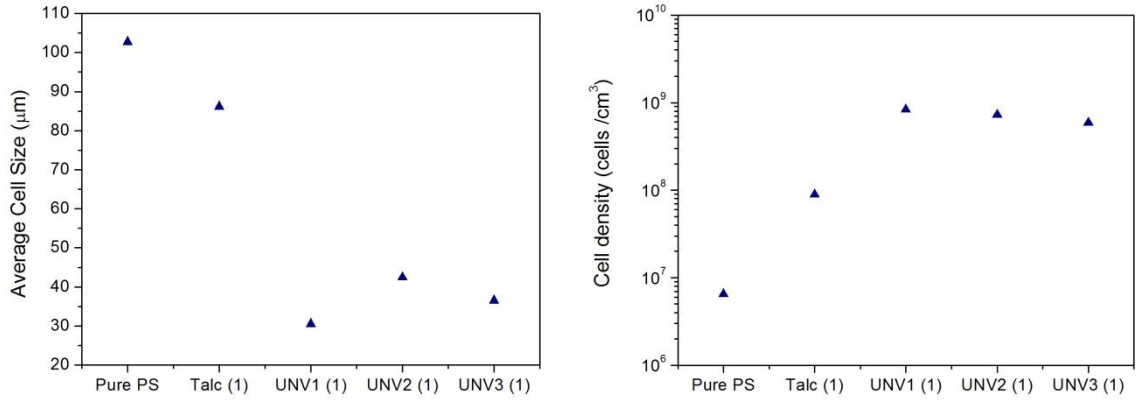

Figure 23: Average cell size and cell density for pure PS and for samples containing 1wt. % of different type of fillers.

Sample	Density (Kg/m^3)	Average Cell Size (µm)	Standard Deviation (µm)	Cell Density ($cells/cm^3$)
Pure PS	40	194.6	29.5	$6.5 \cdot 10^6$
PS + 1% Talc	34	86.2	33.1	$8.9 \cdot 10^7$
PS + 1% UNV-1	52	35.2	14.4	$8.3 \cdot 10^8$
PS + 1% UNV-2	41	42.4	16.1	$7.3 \cdot 10^8$
PS + 1% UNV-3	45	41.6	18.8	$5.8 \cdot 10^8$

Table 5: Main characteristics for pure PS and for samples containing 1wt. % of different type of fillers.

Although the three types of sepiolites produced similar improvements in the cellular structure of PS foams, it was decided to focus the study on the non-treated sepiolite (UNV-1). Figure 24 and Table 6 summarize the effect of increasing the amount of nanoparticles on the cellular structure of the foams.

It can be observed a progressive reduction of the cell size and an increase of cell density. The increase of cell density achieved for the sample containing 5wt. % of sepiolite (two orders of magnitude) is mainly due to the higher nucleation rate obtained when the nanoclays are added, but there is probably another effect related to a better stability of the molten polymer during foaming. It is also observed a bimodal cell size distribution with a few bubbles of larger sizes.

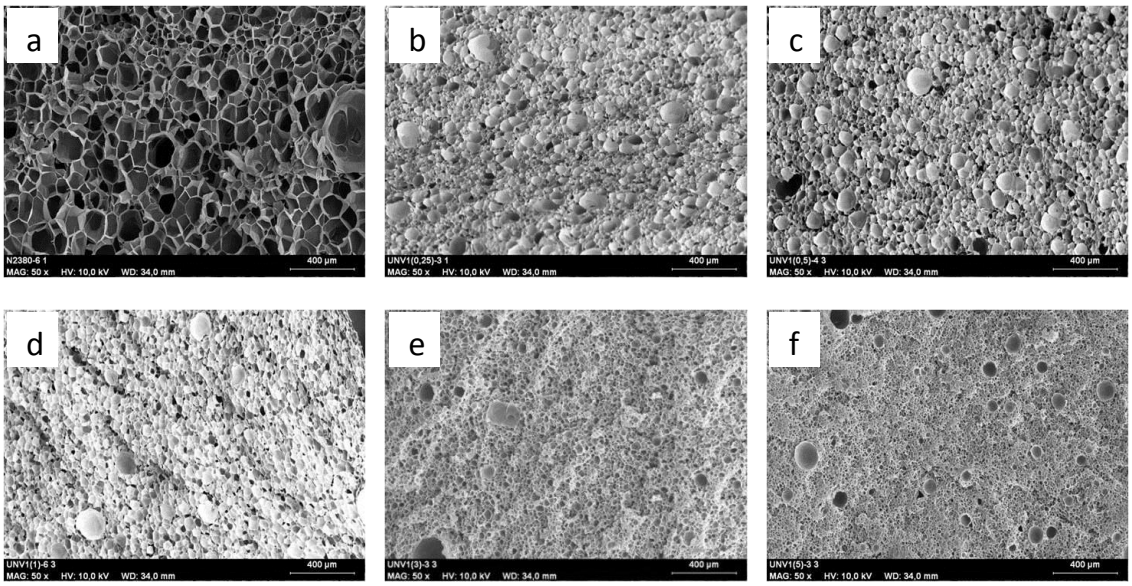

Figure 24: Cellular structure of samples containing different amounts of untreated sepiolite (UNV-1). a) Pure PS, b) 0.25%, c) 0.5%, d) 1%, e) 3%, f) 5%

A reduction of the standard deviation of the cell size is also obtained as well as an increase of the density over the pure polymer.

Sample	Density (Kg/m^3)	Average Cell Size (µm)	Standard Deviation (µm)	Cell Density ($cells/cm^3$)
Pure PS	30	86.16	27.2	$1.01 \cdot 10^8$
UNV-1 0.25%	58	31.17	13.4	$1.07 \cdot 10^9$
UNV-1 0.5%	55	35.30	17.3	$7.84 \cdot 10^8$
UNV-1 1%	52	35.24	14.4	$8.39 \cdot 10^8$
UNV-1 3%	30	21.66	6.5	$6.44 \cdot 10^9$
UNV-1 5%	52	14.17	3.8	$1.31 \cdot 10^{10}$

Table 6: Main characteristics of samples containing different amounts of untreated sepiolite (UNV-1).

Open Cell Content

Open cell content was also measured. Figure 25 shows the results for the systems under study. Once more, sepiolites have a positive effect yielding lower open cell contents than that achieved for the pure polymer or for the conventional solution based on talc. Likewise, the untreated particle gives lower values of open cell content than the treated sepiolites, although the differences are not significant. In addition, it is also observed that as the percentage of non-modified sepiolite increases, this effect is emphasized reaching its minimum value at 3wt. % of nanoclays content. For a 5wt. % the values are similar to that obtained for 1wt. %, which could be associated to a poorer dispersion of the particles when the particles content reached such high values (5wt. %). Moreover, it can be also said that for all the systems closed cell foams are reached due to the low open cell content exhibited by them.

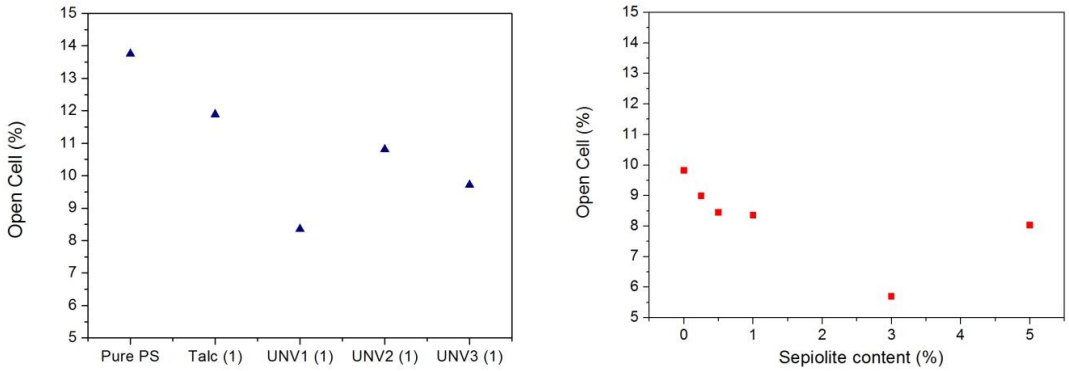

Figure 25: Open cell content of the materials under study. a) Pure PS and foams containing 1wt.% of different fillers. b) Foams containing different amounts of untreated sepiolite (UNV-1)

Thermal Conductivity

Thermal conductivity measurements for the samples containing different amounts of untreated sepiolite are shown in Figure 26. Due to the differences in the foams densities, the values of thermal conductivity have been divided by the foam density to avoid this factor. Only filler contents around 3% have a significant effect in this property. The value for the material containing 1% talc was 0.9 $mW \cdot m^2/Kg \cdot K$. The maximum reductions reached are around 10%. It is well known that thermal conductivity decreases as the cell size does, thus a reduction of thermal conductivity is expected taking into account the strong reduction of cell size shown in Table 6. This reduction on thermal conductivity is very significant, currently the typical values of the thermal conductivity of XPS boards is around 30 to 32 mW/mK; a reduction of 10% would allow producing materials with conductivities in the range of 27 to 28 mw/mK, which is nowadays a key target for XPS producers.

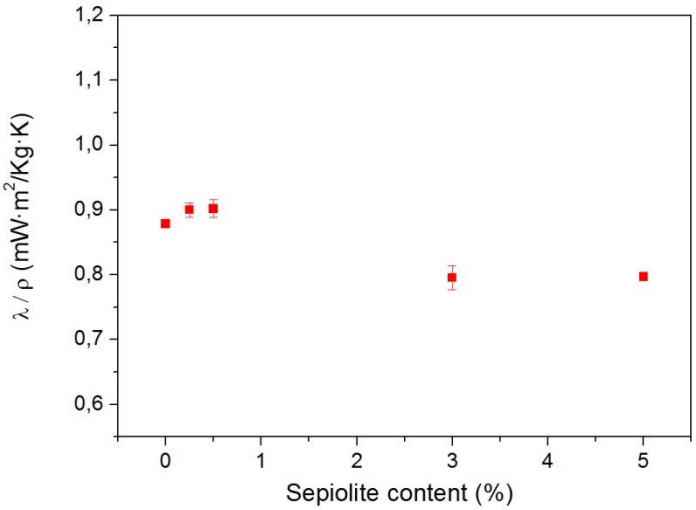

Figure 26: Relative thermal conductivity for the samples containing different percentages of sepiolite UNV-1.

Dispersion of Nanoparticles

As it was explained in Sections 2.2 and 2.3, to reach all the improvements that can be achieved by the addition of nanoparticles, a high degree of dispersion of the same in the polymer matrix is needed. In our case, taking into account the high surface area of the sepiolites, a good dispersion of these nanoparticles could generate a high number of nucleation sites yielding a reduction of the cell size and an increase in the cell density. These two latter are key parameters for reducing the thermal conductivity as well as for improving other properties such as mechanical properties. Results reveal that the addition of sepiolites improves the aforementioned properties, however it is not known if these nanoparticles are well-dispersed or not and consequently, if all its potential is fully exploited.

For this reason, a theoretical model and an experimental methodology have been used (see Section 5.2 for a detailed description of both) with the aim of studying the dispersion of the nanoclays within the polymer matrix. It was decided to focus the study on the untreated sepiolites (UNV-1) at 1wt. % and to use the system containing 1wt. % of talc as a reference.

Figure 27 shows the SEM micrographs at three different magnifications [Figure 27a) low magnification (850x), Figure 27b) medium magnification (2000x) and Figure 27c) high magnification (5000x)] of the solid composite for the system containing 1wt. % of talc. Talc particles can be identified as the bright lines or as the black ones which corresponds to the presence or absence of the particle of talc respectively. From Figure 27 it can be inferred that apparently talc is well-dispersed and well-distributed, although some agglomerates are present.

On the other hand, the SEM micrographs with backscattered electrons corresponding to the solid nanocomposites containing 1wt. % of non-modified sepiolites at four different magnifications are shown in Figure 28 [Figure 28a) low magnification (500x), Figure 28b) and Figure 28c) medium magnifications (4000x and 10000x respectively) and Figure 28d) high magnification (30000x)]. Sepiolite particles can be appreciated in the micrographs as the bright spots. It can be deduced from this figure that sepiolites in principle are not individually dispersed but forming well-distributed aggregates.

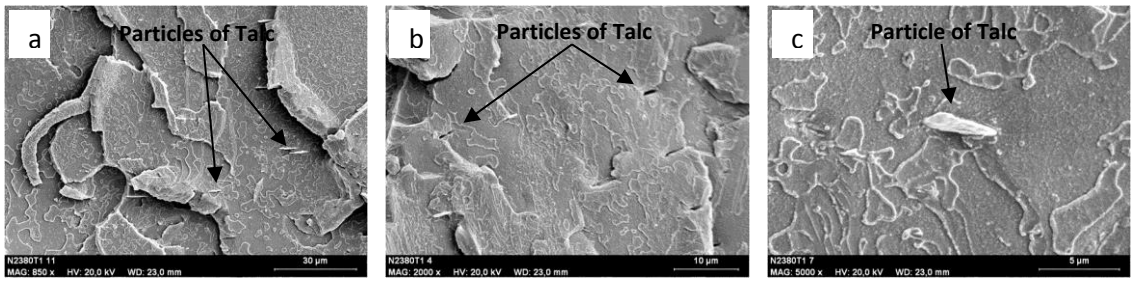

Figure 27: Solid composite containing 1wt. % of talc at different magnifications. a) 850x, b) 2000x, c) 5000x.

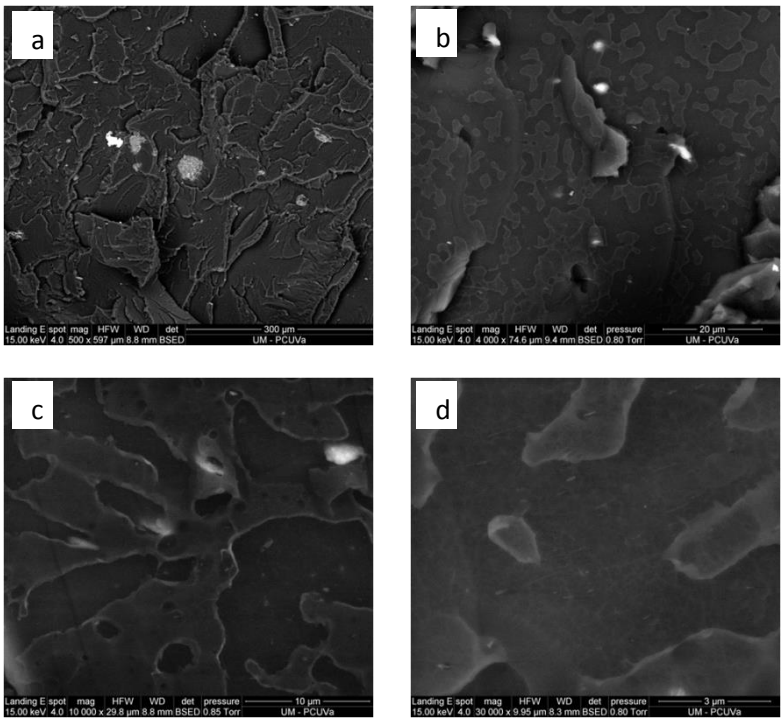

Figure 28: Solid nanocomposites containing 1wt. % of untreated sepiolites (UNV-1) at different magnifications. a) 500x, b) 4000x, c) 10000x, d) 30000x.

The mere observation of the images does not lead to any conclusion about the effect of the particles in the polymer matrix and, consequently, in the subsequent cellular structure. Therefore it is necessary to perform a quantitative analysis.

The number of particles per unit of volume was the first parameter analyzed. The results calculated by Eq. 4 together with the ones obtained via experimental methodology are represented in Figure 29 for the different magnifications. It is observed that talc presents a possible number of nucleation sites lower than sepiolite due to its larger size. This justifies some of the aforementioned results where the cell density in the case of talc was lower than in the case of sepiolites (Table 5).

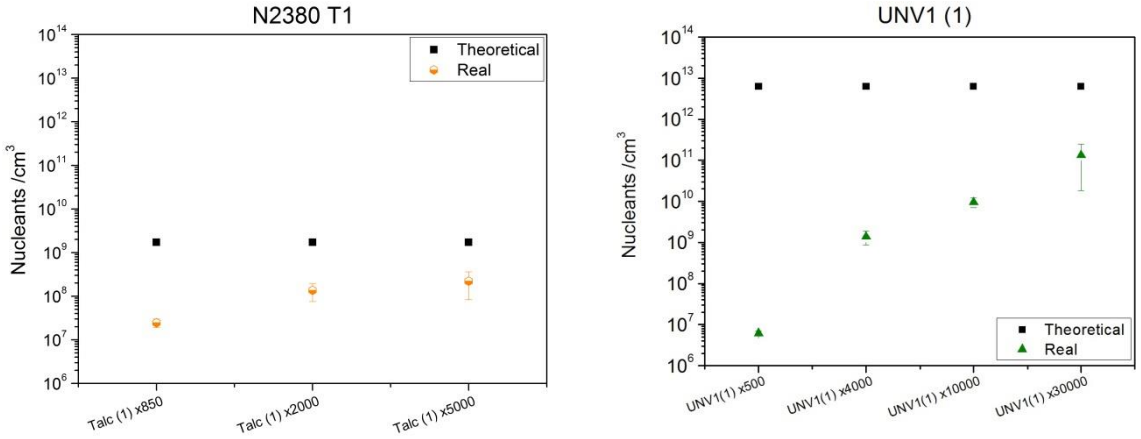

Figure 29: Number of nucleants per unit volume calculated using both methodologies both for the talc and for the untreated sepiolites at the different magnifications.

Figure 30 shows the agglomeration ratio for both foams containing talc and the untreated sepiolite (UNV-1). Values were calculated for the different magnifications in both cases. Significant differences are observed again between both systems. The number of talc particles per agglomerate are lower than the number of sepiolite particles per agglomerate suggesting that talc particles seem to be well-dispersed or at least better dispersed than sepiolite ones.

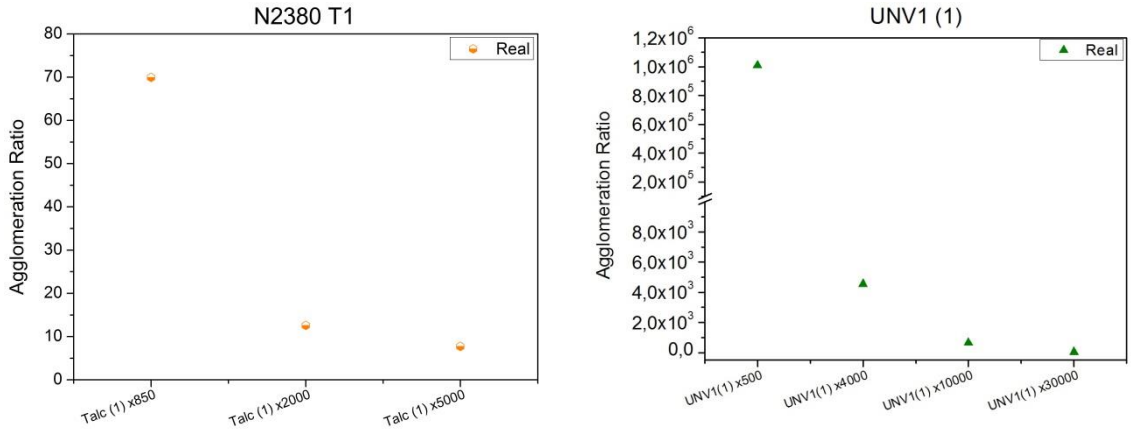

Figure 30: Agglomeration ratio for the reference system (talc) and for the non-modified sepiolites (UNV-1) for the different magnifications

Nucleation efficiency was calculated for each system at the different magnifications and results are shown in Figure 31. In the case of talc, both theoretical and experimental values are close to one so that talc seems to be acting as a good nucleating agent due to an apparent good dispersion of the particles. With respect to sepiolites, low theoretical values suggest that these particles seem to not be effective nucleating agents. On the other hand, observing the experimental values, agglomerates seem to be the effective nucleating agents against what Figure 22 shows where cells are very small. These cells cannot be formed from such large agglomerates. Thus it is not known who is acting as effective nucleating agent, if the agglomerates or the individual particles, and in addition, it cannot be concluded if sepiolites act or not as an effective nucleating agent.

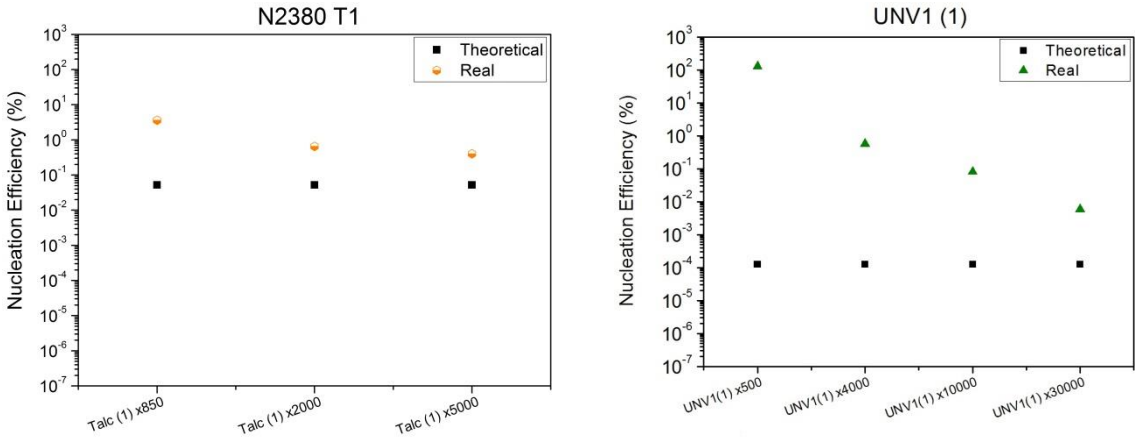

Figure 31: Nucleation efficiency for the systems under study at the different magnifications.

It is remarkable that for all the calculated parameters the obtained results are different depending on the magnification, being these differences greater in the case of the untreated sepiolite. The reason that lies behind this could be explained as follows: talc particles are bonded by weak Van der Waals forces so when they are melt blended with the polymer, the shear mixing forces are enough to separate them obtaining a good dispersion of talc particles within the polymer matrix although some agglomerates are still formed. Differences in magnification are not too large, so it could be inferred that talc particles are well-dispersed and well-distributed because at all scales we are observing the same.

Regarding to sepiolites, their natural state is to be agglomerated due to their large surface energy. Possibly shear mixing forces are not sufficient to separate them. Likewise, the fact that the differences in magnification are so big that it suggests they are probably not well-dispersed. However, with these results, it can only be assured that there are some agglomerates and some individual particles without knowing which of the two predominates. Therefore, it would be necessary to go one step further in the study to know the true distribution of the particles that will allow us to relate the latter with the final cellular structure.

7. CONCLUSIONS

In-situ characterization of the foaming process in PE/ MMT system

Synchrotron radiation has turned to be a very useful in-situ technique to take an insight into the mechanisms involved in the increment of the exfoliation degree of LDPE/clay nanocomposites during foaming using chemical blowing agents. The whole evolution of the process has been characterized.

Three blowing agents were selected. Two of them release gas but different in between, one mainly nitrogen and the other one mainly CO_2. In the case of the third blowing agent the gas remains confined within the microspheres being the swelling of these microspheres what produces the foaming. The increment of interlamellar spacing while foaming occurs is independent of the blowing agent used. Thus the phenomenon is related to the foaming itself and not with the kind of gas or foaming procedure used.

The blend nanoclays/azodicarbonamide yields higher exfoliation degrees during mixing. Therefore a chemical interaction between azodicarbonamide and organomodified nanoclays is postulated. This chemical interaction helps to the clays delamination during blending. On the contrary the blend with hydrocerol or expancel does not have any effect on the exfoliation. These latter samples present an exfoliation state similar to the one achieved when the blending is performed without any blowing agent.

The increment in the interlamellar distance is not only carried out by the foaming but also by the thermal mobility of the polymer molecular chains. The movement of the polymer chains bonded to the edges of the nanoclays platelets separates them and contributes to their disorder. This effect is observed independently of the foaming agent nature or nanoclays content.

There is a correlation between expansion ratio and increment in interlamellar distance. The higher increments in exfoliation degree are found in the samples with lower densities. This effect has been observed both with ex-situ and in-situ XRD and using different systems. For all the samples a maximum interlamellar spacing is reached during the foaming. In the case of the azodicarbonamide samples this maximum interlamellar distance is conserved after foam collapse and solidification. On the contrary, in the samples containing expancel and hydrocerol the exfoliation degree found after collapse and solidification is lower than the maximum observed. The postulated interaction azodicarbonamide-nanoclays may help to keep the nanoclays platelets hooked to their new positions reached during the foaming.

Higher additions of nanoclays help to achieve lower densities in free foaming. Several reasons have been hypothesized to explain this result. Again the higher is the expansion ratio obtained; the higher is also the increment in the interlamellar spacing.

This scientific work has shown a new experimental methodology for following in-situ the exfoliation process of nanoclays. Foaming, by itself, promotes the separation degree between platelets in a nanoclay-filled composite.

Characterization of dispersion in the PS/ Sepiolite system

Sepiolite is a very promising additive for the production of low density PS foams. The addition of small contents of these nanoparticles can lead to significant improvements in cellular structure of PS based foam (lower cell size, higher cell density, higher cell size homogeneity and lower open cell content).

The three types of sepiolites used allow reducing significantly the average cell size in the materials in a similar extend. Cell size is reduced in a factor 2 or 3 for high particle content, increasing the cell density in at least one order of magnitude for low particle content and in two orders of magnitude for high particle content. This take place both when compared with the structure of the pure polystyrene as with the structure of the material that uses the most common nucleating agent, talc. In addition, nanoparticles tend to generate structures with lower open cell contents.

The reason for this significant improvement in the structure of the materials could be due to:

- A higher number of nucleation sites in the materials containing sepiolites and/ or a more effective action of sepiolites as nucleating agent.
- An improvement in the rheological behavior (extensional viscosity) of the materials infused with sepiolites.
- A combination of both effects.

Thermal conductivity is also improved. Higher contents (3wt. %) allow reducing in a significant extend (up to 10%) the thermal conductivity of the system. This remarkable reduction is a key factor for manufacturers of XPS who are dealing with conductivities around 30-32 mW/mK.

The dispersion and distribution of the particles within the polymer matrix is acceptable. Talc particles seem to be well-dispersed and well-distributed, although some agglomerates are present. Their nucleation efficiency both theoretical as experimental is close to one so it is acting as an efficient nucleating agent. This effectiveness justifies that talc is so used as nucleating agent in polystyrene as well as in another systems. With respect to non-modified sepiolites, both agglomerates as individual particles have been detected without knowing which of the two predominates. The number of particles per unit of volume in the case of sepiolites is higher than that in talc due to its smaller size. This could be the explanation of the better behavior than talc as nucleating agent for this particular system.

The used methodologies for the study do not lead to any further conclusion revealing the requirement of another methodology that let us quantify the real dispersion of the system.

On the other hand, the surface treated particles used in this study promoted a similar effect than the non-treated ones.

As a general conclusion of the performed investigations we could say that sepiolites are clearly superior to talc as additives to improve the structure and properties of PS foams since an adequate selection and dispersion of the same in the polystyrene matrix allow manufacturing materials with better properties.

Therefore the use of these materials as additives in foaming processes has a great marketing potential, however there is still a significant gap for improvement if a better dispersion is reached.

8. FUTURE WORK

In-situ characterization of the foaming process in PE/ MMT system

An investigation focused on obtaining a better understanding of the mechanisms that induce the exfoliation of nanoclays during the foaming processes of low density polyethylene (LDPE)/clays nanocomposites is going to be performed. Beamtime has been allocated for our project from 23rd to 26th of January, 2014.

Nanocomposites of a LDPE containing different amounts of nanoclays (montmorillonite (MMT)) and a chemical blowing agent (azodicarbonamide) will be prepared by using melt mixing. Three different types of clays with different surface treatments will be used.

The analysis of these experiments will provide further insight on the mechanisms promoting the exfoliation of nanoclays during foaming and on the effect of the nanoparticles on the mechanisms (nucleation, growth and coalescence) taking place during foaming.

Characterization of dispersion in the PS/ Sepiolite system

A new methodology for a real quantification of the number of particles that are forming agglomerates is being developed. It is going to be also applied to different contents of non-modified sepiolite (UNV-1). To corroborate the validity of this methodology, we will study other systems containing nanoparticles with a different shape with respect to sepiolites and we will use other techniques such as SAXS or microtomography. Knowing the dispersion of the nanoclays, it is possible to get better improvements and therefore to obtain properties never achieved before.

A parallel study to the one performed with sepiolites UNV-1 will be carried out using sepiolites treated with silanes (UNV-3) with the aim of elucidating if the surface treatment with silanes has or not any influence in the dispersion of these nanoparticles and consequently in the final cellular structure of PS based foams.